International Journal of Pharmaceutics 604 (2021) 120711

Contents lists available at ScienceDirect

International Journal of Pharmaceutics

journal homepage: www.elsevier.com/locate/ijpharm

Microfluidic-assisted fabrication of phosphatidylcholine-based liposomes for controlled drug delivery of chemotherapeutics

Leonidas Gkionis [a], Harmesh Aojula [a], Lynda K. Harris [a,b,c], Annalisa Tirella [a,*]

[a] Division of Pharmacy and Optometry, Faculty of Biology, Medicine and Health, University of Manchester, Manchester Academic Health Science Centre, Oxford Road, Manchester M13 9PL, United Kingdom
[b] Maternal and Fetal Health Research Centre, Division of Developmental Biology and Medicine, Faculty of Biology, Medicine and Health, University of Manchester, 5th floor (Research), St Mary's Hospital, Oxford Road, Manchester M13 9WL, UK
[c] St Mary's Hospital, Manchester University NHS Foundation Trust, Manchester Academic Health Science Centre, Manchester M13 9WL, UK

ARTICLE INFO

Keywords:
Phosphatidylcholine
Binary liposomes
Microfluidics
Doxorubicin
Drug delivery
Nanomedicine

ABSTRACT

Microfluidic enables precise control over the continuous mixing of fluid phases at the micrometre scale, aiming to optimize the processing parameters and to facilitate scale-up feasibility. The optimization of parameters to obtain monodispersed drug-loaded liposomes however is challenging. In this work, two phosphatidylcholines (PC) differing in acyl chain length were selected, and used to control the release of the chemotherapeutic agent doxorubicin hydrochloride, an effective drug used to treat breast cancer. Microfluidics was used to rapidly screen manufacturing parameters and PC formulations to obtain monodispersed unilamellar liposomal formulations with a reproducible size (i.e. < 200 nm). Cholesterol was included in all liposomal formulations; some formulations also contained DMPC(1,2-dimyristoyl-*sn*-glycero-3-phosphocholine) and/or DSPC(1,2-distearoyl-*sn*-glycero-3-phosphocholine). Systematic variations in microfluidics total flow rate (TFR) settings were performed, while keeping a constant flow rate ratio (FRR). A total of six PC-based liposomes were fabricated using the optimal manufacturing parameters (TFR 500 μL/min, FRR 0.1) for the production of reproducible, stable liposome formulations with a narrow size distribution. Liposomes actively encapsulating doxorubicin exhibited high encapsulation efficiencies (>80%) for most of the six formulations, and sustained drug release profiles *in vitro* over 48 h. Drug release profiles varied as a function of the DMPC/DSPC mol content in the lipid bilayer, with DMPC-based liposomes exhibiting a sustained release of doxorubicin when compared to DSPC liposomes. The PC-based liposomes, with a slower release of doxorubicin, were tested *in vitro,* as to investigate their cytotoxic activity against three human breast cancer cell lines: the non-metastatic ER+/PR + MCF7 cells, the triple-negative aggressive MDA-MB 231 cells, and the metastatic HER2-overexpressing/PR + BT474 cells. Similar cytotoxicity levels to that of free doxorubicin were reported for $DMPC_5$ and $DMPC_3$ binary liposomes (IC_{50} ~ 1 μM), whereas liposomes composed of a single PC were less cytotoxic (IC_{50} ~ 3–4 μM). These results highlight that microfluidics is suitable for the manufacture of monodispersed and size-specific PC-based liposomes in a controlled single-step; furthermore, selected PC-based liposome represent promising nanomedicines for the prolonged release of chemotherapeutics, with the aim of improving outcomes for patients.

1. Introduction

The structure–function relationships of biological membranes have been studied for decades using model membranes. The lipid clusters in all cell membranes, at physiological temperatures, present as an equilibrium ratio of gel and fluid phases that determine the ultimate dynamics of the membrane trafficking properties (Kapitza et al., 1984; Peetla et al., 2009). Liposomes are artificial, hollow vesicular structures; their lipid bilayer is similar to that of biological membranes, consisting of natural and/or synthetic phospholipids usually combined with cholesterol (Akbarzadeh, 2013; Juszkiewicz et al., 2020). Permeability is an important physical attribute of liposomes, since it determines the diffusion rate of encapsulated compounds throughout the lipid bilayer when used for therapeutic applications (Chen et al., 2018). Near their liquid-crystalline transition temperatures, liposomes become highly leaky to their hydrophilic entrapped contents (Chen, 2013; Lokerse,

* Corresponding author.
E-mail address: annalisa.tirella@manchester.ac.uk (A. Tirella).

https://doi.org/10.1016/j.ijpharm.2021.120711
Received 23 April 2021; Received in revised form 11 May 2021; Accepted 12 May 2021
Available online 18 May 2021

2016), a phenomenon generally attributed to disorder at the boundaries between gel and fluid domains in the lipid clusters. This thermodynamic property along with the existing environmental conditions (e.g. pH, ionic strength, enzymatic degradation, plasma proteins association) ultimately determine the circulation time of liposomal carriers into the bloodstream, as well as their ability to extend retention of the entrapped solutes (Abri Aghdam, 2019).

The equimolar (1:1) binary mixture of DSPC/DMPC phospholipids has so far been one of the most thoroughly investigated two-component bilayer model, both experimentally and theoretically since the 1980 s (Koynova and Caffrey, 1998). However, no recent studies have attempted to elucidate further the thermomechanical properties of this otherwise, non-ideal colloidal system, by incorporating 30–35% cholesterol into the final lipid composition, while keeping the % DSPC molar content within a narrow range and under acceptable thermodynamic limits that typically do not exceed the 20% molar ratio (Michonova-Alexova and Istvan, 2002). Cholesterol is largely known to affect the fluidity of both natural and synthetic bilayers. This steroid molecule acts as a stabilizer, which directly impacts the viscoelasticity of the lipid bilayer; it increases the mechanical stiffness (mainly the packing order) while allowing membrane fluidity (Briuglia et al., 2015; Kirby et al., 1980). This is of particular importance in fluid-like bilayers, where cholesterol can offer improved rigidity by filling the free space in the layer and reducing the mobility of the surrounding lipid chains (Bhattacharya and Saubhik, 2000; Soto-Arriaza et al., 2013). Moreover, cholesterol is known to reduce the leakage of soluble, hydrophilic drugs across the lipid bilayer (Raffy and Teissié, 1999), as well as promote drug loading in liposomes (Farzaneh et al., 2018). In the case of doxorubicin-loaded liposomes for example, cholesterol has been assumed to enhance doxorubicin transport across the lipid bilayer by moderating the hydrophobic character of the compact lipid membrane, especially when consisted of long-tail saturated phospholipids like DSPC or DPPC (Farzaneh et al., 2018). Interactions of cholesterol with multicomponent lipid systems are often difficult to predict, e.g. perplexed fluid-like and liquid-ordered phases (Soto-Arriaza et al., 2013).

In our previous work, we reported the manufacturing of PEGylated phosphatidylcholine (PC) and cholesterol liposomes using microfluidics, by varying the lipid concentration feed in the organic phase. We reported that microfluidic technology replicates bulk methods (e.g. rehydration methods, solvent injection induced protocols (Shah et al., 2020) and fabricates liposomes with a defined geometry and size, offering also precise control over various manufacturing parameters. Microfluidics ultimately allows fast, high-throughput manufacturing and provides a robust and reproducible method for the fabrication of liposomes and other types of nano-formulations (Carugo et al., 2016; Feng, 2018; Chiesa, 2020).

In the current study, we evaluated the impact of using different lengths of PCs on the characteristics of liposomes manufactured using microfluidics. Dimyristoyl phosphatidylcholine (DMPC) and distearoyl phosphatidylcholine (DSPC) were selected, and liposomes manufactured using fixed lipid concentrations of either DMPC:Chol or DSPC:Chol lipid compositions, as well as their binary mixtures. The manufacturing steps were optimised to fabricate small, unilamellar and monodispersed liposomes with target size of 80–150 nm. The physicochemical properties of produced liposomes were characterised, as to validate the efficacy of the manufacturing process (e.g. lipid content, transition temperature shifting, morphology, size, drug loading). Additionally, stability (storage conditions) and drug release profiles were investigated in order to elucidate the impact of PCs on drug release profiles and enable sustained release.

Doxorubicin was selected as a hydrophilic model drug, while being the main representative antineoplastic agent of the anthracycline antibiotics family (Cortés-Funes and Coronado, 2007). Doxorubicin is extensively used for the clinical treatment of breast cancer (Swain, 2013), with examples of doxorubicin-loaded liposomes being already used clinically (Khan et al., 2015; Belfiore, 2018). The ionisable properties of doxorubicin enable the use of a transmembrane pH-gradient loading method, which provides high drug loading and minimal drug diffusion rates from the liposomal carriers (Haran et al., 1993; Sur et al., 2014). The most successful example is the commercial product Doxil®, which encapsulates>90% of doxorubicin at maximal dose of 2 mg/mL (Barenholz, 2012), while retaining a circulation half-life time of about 90 h. Doxorubicin leakage from Doxil® liposomes has been evaluated to be<20% over a period of 120 h exposure, under sink conditions resembling human physiology (Russell et al., 2018; Shibata et al., 2015).

Among the produced DMPC/DSPC mixed liposomal formulations, we selected and reported the ones with doxorubicin release profiles of $\leq$ 50% within the first 24 h. Cytotoxicity of selected liposomes was tested against three human breast cancer cell lines: the non-metastatic oestrogen- and progesterone-positive (ER+/PR +) MCF-7 cells, the triple-negative aggressive MDA-MB 231 cells, and the highly metastatic HER2-overexpressing/PR + BT-474 cells. The different physicochemical features of the liposomes, as well as the unique release pattern of each formulation, resulted in different cytotoxic patterns against the cancer cells tested. We found that mixed liposomes using PCs and cholesterol can be fabricated using microfluidics, with high control over liposomes properties. The effect of lipid composition and drug membrane partitioning ultimately governs the release rate of the encapsulated chemotherapeutic, thus determining the future therapeutic scheme of selection (such as dose and administration) for each liposomal carrier.

2. Experimental section

2.1. Materials

1,2-distearoyl-*sn*-glycero-3-phosphocholine (DSPC 18:0, Product Number 850365P), 1,2-ditetradecanoyl-*sn*-glycero-3-phosphocholine (DMPC 14:0, Product Number P2663) and 1,2-distearoyl-*sn*-glycero-3phosphoethanolamine N-[methoxy(polyethylene glycol)-2000] ammonium salt (DSPE-PEG2000-PE, Product Number 880120P) were obtained from Avanti Polar Lipids (Alabaster, AL). Cholesterol (Chol, C8667), ammonium sulphate (A4418), ferric chloride hexahydrate (236489), ammonium thiocyanate (221988), phosphate buffer saline (PBS, P4417), 4-(2-Hydroxyethyl)piperazine-1-ethanesulfonic acid, N-(2-Hydroxyethyl) piperazine-N′-(2-ethanesulfonic acid) (HEPES, H4034), sodium chloride (S9888), doxorubicin hydrochloride (D1515) and methanol (HPLC grade) were purchased from Sigma-Aldrich, Gillingham, UK. Chloroform and Acetonitrile (HPLC grade) were obtained from Fisher Scientific, Loughborough, UK.

All liposomal formulations were prepared with different DSPC/DMPC molar ratio and included 3% mol DSPE-PEG_{2000} (Table 1); hence, thereafter they are referred to as liposomes.

2.2. Production of liposomes using a microfluidic system

Liposomes were prepared using the automated Dolomite

Table 1
Organic phase lipid compositions for the preparation of liposomes in pure methanol.

Liposomes	Lipid Composition DSPC (mg/mL)	DMPC (mg/mL)	Cholesterol (mg/mL)	DSPE-PEG2000 (mg/mL)	Molar ratio (%) DSPC:DMPC: Chol:DSPE-PEG2000-PE
$DMPC_{100}$	–	10	3	3	0:64:33:3
$DMPC_{10}$	1	9	3	2	5:58:34:3
$DMPC_5$	2	8	3	2	11:52:34:3
$DMPC_3$	3	8	3	2	16:49:32:3
$DMPC_{0.2}$	11	2	3	2	57:11:29:3
$DSPC_{100}$	10	–	2.5	1.8	64:0:33:3

microfluidic system (Dolomite, Royston, UK) equipped with the 3-Input Chip (Part No. 3200735). The aqueous phase (i.e., HEPES saline buffer) was prepared dissolving 150 mM NaCl and 20 mM HEPES in ultrapure water, with the pH value adjusted to 7.4 using 0.1 N HCl. The organic phase was prepared by mixing different molar ratios of DMPC, DSPC, Chol, and DSPE-PEG2000-PE in pure methanol (as reported in Table 1). Both aqueous and organic solutions were filtered twice through 0.22 μm PVDF filters (Millex-CV, Merck Millipore Ltd. Germany) prior to each experiment, and discarded after use. During all the experiments, the temperature of DMPC-containing solutions and chip was set and maintained at (40 ± 1)℃ using a hotplate stirrer (IKA, Germany), and the back pressure of the microfluidic system was set at 2 bars. Only $DSPC_{100}$ liposomes were fabricated at (60 ± 1)℃ because of the higher phase transition temperature of this lipid.

Based on our previous study (Gkionis et al., 2020), the flow rate ratio (FRR), defined as the volumetric ratio of the aqueous phase stream to the organic phase stream, was set to 1:10 to obtain reproducible, monodisperse and uniform unilamellar liposomes. The total flow rate (TFR) was used as a manufacturing variable to optimize liposome size, size distribution and shape.

A typical experiment was performed collecting a final liposomal formulation volume of 3–5 mL, with the possibility of scaling-up the production to volumes of ≥ 20 mL. A volume of 2 mL was sampled and transferred to Float-A-Lyzer G2 (Biotech CE, 3.5–5 kDa MWCO, 1 mL), then dialyzed against 1 × PBS solution for 16 h at RT (buffer exchanged every 4 h) for removal of any residual solvent or free drug.

2.2.1. Viscosity measurements

The viscosity of $DMPC_{100}$ and $DPSC_{100}$ organic phases was measured using the AMVn Automated Microviscometer (Anton Parr, UK) and calculated considering the flying time taken of a gold ball to move in a glass capillary filled with the solution to test. Two capillaries of diameter 1.6 mm and 1.8 mm were used for the measurement with a 1.5 mm diameter gold ball (7.83 g/cm^2 density). Measurements were performed at 25℃ and 40℃ (n = 3 independent samples).

2.2.2. Drug-free liposomes

The manufacturing of drug-free liposomes was optimized using $DMPC_{100}$ and $DPSC_{100}$ organic phases (for composition refer to Table 1), by varying the TFR between 250 and 750 μL/min. During all the experiments, the FRR was set to 1:10; the temperature of aqueous and organic phases, as well as tubing and chip, was set to 40℃ or 60℃ respectively.

2.2.3. Drug-loaded liposomes

Doxorubicin-loaded liposomes were prepared using the previously optimized fabrication parameters (TFR 500 μL/min, FRR 1:10, 40 or 60℃) and different lipid formulations were used as the organic phase (Table 1). Doxorubicin hydrochloride was loaded into liposomes using the pH gradient-mediated method with 250 mM ammonium sulphate buffer (pH adjusted to 5.1–5.4) used as the aqueous phase (Gkionis et al., 2020). Prior to manufacturing, all solutions were filtered twice using a 0.22 μm PVDF filter. After preparation and dialysis to remove any impurities (3 h, RT, Float-A-Lyzer G2, 3.5–5 kDa MWCO), liposomes were incubated with 0.2 mg/mL doxorubicin solution for 2 h at 60℃. Samples were further dialyzed against 1 × PBS solution (16 h, RT, Float-A-Lyzer G2, 3.5–5 kDa MWCO) and stored at 4℃ until further use. All samples were discarded after 2 weeks storage.

2.3. Physicochemical characterization of liposomes

2.3.1. Lipid quantification: Steward assay

The total amount of lipids in liposomal formulations was measured via Steward assay (Charles and Stewart, 1980), using ammonium ferrothiocyanate reagent to bind with the phospholipid head groups in an emulsion of 1:1 (v/v) water:chloroform. Pure chloroform was used as a reference sample. Briefly, 27.03 g of ferric chloride hexahydrate and 30.4 g of ammonium thiocyanate were dissolved in 1 L of distilled water. A volume of 20 μL of the lipid sample was added to 980 μL of chloroform, followed by addition of 1 mL of ammonium ferrothiocynate reagent. The mixture was vortexed and then centrifuged at 1000 rpm for 15 min at RT. The chloroform layer was transferred to a glass cuvette, where absorbance measured at 485 nm (Perkin Elmer Lambda 3B UV–VIS, UK) was read. A calibration curve in the range of 0.01–0.125 mg/mL of DMPC or DSPC lipid (*Supplementary Information, Fig SI.1 and Fig SI.2*) was obtained and used to calculate the lipid concentration of each formulation.

2.3.2. Dynamic light scattering

Liposome size, measured as hydrodynamic diameter (Z-average size), polydispersity and surface charge (ξ-potential) were measured by dynamic light scattering using a Zetasizer Nano ZS (model ZEN3600, Malvern Instruments Ltd., UK) equipped with a solid state HeNe laser (λ = 633 nm) at a scattering angle of 173°. All samples were tested at 25℃ (pre-equilibration for 2 min) in HEPES buffer saline and without any additional dilution. Liposome size distributions were calculated by applying the general-purpose algorithm and presented as the average of the Z-average values of three independent preparations (n = 3).

2.3.3. Drug loading and encapsulation efficiency

The amount of doxorubicin hydrochloride loaded in liposomal formulations was quantified using a Perkin Elmer Series 200 HPLC system equipped with a C18 reverse-phased column (ACE™, 5 μm particle size, 150 × 4.6 mm i.d., Hichrom Ltd, Berkshire, UK). Samples were eluted using a 30 min linear gradient of acetonitrile (80:20 ACN:H_2O, 0.1% v/v TFA) and ultrapure distilled water (100%, 0.1% v/v TFA), with the flow rate, injection volume and detection wavelength set at 1 mL/min, 50 μL, and 260 nm respectively. The doxorubicin peak was detected at 11 min. Doxorubicin solutions in the concentration range of 2–35 μg/mL were diluted in 0.1% v/v TFA solution (aq.) and used to obtain a linear calibration curve.

Drug loading (DL%, Eq. (1)) and encapsulation efficiency (EE%, Eq.2) were calculated for each preparation (n = 3).

$$DL(\%) = \frac{\text{mass of drug loaded}}{\text{total weighted lipid mass}} x100 \quad (1)$$

$$EE(\%) = \frac{\text{amount of drug encapsulated}}{\text{total drug added}} x100 \quad (2)$$

2.3.4. Drug release studies

Doxorubicin release was measured using the dynamic dialysis method under sink conditions (Shibata et al., 2015). A volume of 2 mL of doxorubicin-loaded liposomes (already purified from any free drug presence via dialysis) was added to a dialysis cassette (MWCO 3.5 kDa, 0.5–3 mL, Prod no. 66330, ThermoFisher Scientific) and dialyzed against 400 mL of 1 × PBS buffer (pH 7.4). Drug release studies were performed at 4℃ and 37℃. The dialysis cassette was shaken at 100 rpm in a Thermoshaker chamber (New Brunswick™ Innova® 44, Eppendorf UK). A volume of 0.1 mL of liposomes was sampled from the dialysis cassette at selected time points (i.e., 2, 4, 6, 24 and 48 h) and then diluted with cold methanol solution (-20℃) for further analysis with RP-HPLC.

2.3.5. Morphological characterization using transmission electron Microscopy (TEM)

A volume of 3 μL of each liposomal formulation was fixed on glow discharged (25 mA, 1 min) carbon film mesh copper grids using 50 μL of aqueous solution containing 2% v/v uranyl acetate stain (negative staining) for 5 min. Grids were allowed to dry for 15 min at RT prior to acquisitions. Images of independent liposomal preparations (n = 3, N = 3) were acquired using a transmission electron microscope (TEM, FEI

Tecnai 12 BioTwin) operated at an accelerating voltage of 100 kV.

2.3.6. Characterization of liposome size distribution by TEM image analysis

Liposome size distribution was measured using the acquired TEM images. Images ($n \geq 3$) of each formulation were analyzed using ImageJ (Schneider et al., 2012). Briefly, the area of liposomes was detected and measured using the shape descriptors plug-in (counting $\geq$ 200 liposomes). The mean diameter of the liposomes was calculated assuming liposomes as circles, where liposomes with a roundness < 0.8 were excluded from the analysis. Liposome size distribution was analyzed using GraphPad Prism 7, setting 10 nm bin and the Gaussian fit function was used to calculate mean diameter and standard deviation.

2.3.7. Differential scanning calorimetry (DSC)

The glass transition temperature of all liposomes was measured using the differential scanning calorimetry (DSC) with the TA Instruments Q100 DSC Calorimeter (Waters, UK), equipped with a 50-position autosampler. All formulations were freeze-dried before analysis, yielding a 200 mg dry lipid cake. For each formulation, samples were weighed and 2–10 mg were transferred to standard aluminium pans (P/N: 900794.901, TA instruments, Waters, UK). The pans were hermetically sealed and immediately used. The calorimetric analysis was set-up with heating scans from −20℃ to 100℃ and scan rate of 5℃/min. The calorimetric scans were repeated three times ($n = 3$) sequentially to verify the reproducibility of the method. Three independent samples ($n = 3$, $N = 3$) were tested for each preparation.

2.4. Cell culture

Dulbecco's Modified Eagle's medium (DMEM, D6429), fetal bovine serum (FBS, F9665), trypsin (T3924), L-glutamine (G7513), antibiotics (penicillin − streptomycin, P0781) and (3-(4,5-Dimethylthiazol-2-yl)-2,5-Diphenyltetrazolium Bromide) (MTT, M2128) were purchased from Sigma-Aldrich (Gillingham, UK). Human breast adenocarcinoma cell lines MCF-7 (HTB-22™), MDA-MB-231 (HTB-26™) and ductal carcinoma BT-474 (HTB-20™) were kindly donated from Manchester Cancer Research labs (University of Manchester, UK). Unless otherwise specified, all cell culture experiments were performed in a humidified 5% (v/v) CO_2 air atmosphere at 37℃ in complete medium. Cell culture growth medium was supplemented with 10% (v/v) fetal bovine serum, 2 mM L-glutamine, and 1% (v/v) of antibiotics. Human breast adenocarcinoma cell lines were cultured and maintained at densities lower than 1×10^6 cells/mL, and discarded upon reaching passage number 60.

2.4.1. Cytotoxicity assay

MCF-7 and MDA-MB-231 cells were seeded in 96-well plates (3799, Corning Inc., NY, USA) at a density of 10,000 cells/cm^2, and left to adhere overnight, prior to experiments. BT-474 cells were seeded respectively in 96-well plates at a density of 6,700 cells/cm^2 and left adhere overnight prior to experiments. Stocks of doxorubicin hydrochloride were dissolved in ultrapure water at a concentration of 4 mg/mL, filtered through 0.22 μm PVDF filters (Millex-CV, Merck Millipore Ltd. Germany), and then stored at −20 °C until further use. The doxorubicin sterile stock solution was diluted in complete media prior each experiment to concentrations of 0.017, 0.17, 0.85, 1.7, 8.5, 17, 85 and 155 μM (or 0–90 μg/mL). Cells were incubated with doxorubicin dilutions for 48 h (37℃, 5% CO_2).

Drug-free and drug-loaded liposomes were sterile filtered using a 0.22 μm PVDF filter, diluted in complete media at a concentration range of 10–500 μg phosphatidylcholine lipid/mL and incubated with cells for 48 h, based on our previous findings (Gkionis et al., 2020). Doxorubicin-loaded phosphatidylcholine liposomes were diluted in order to incubate cells with the same concentration of doxorubicin. The highest concentration of doxorubicin in liposomes was set to 155 μM. Of note, at this doxorubicin concentration, none of the liposomes tested had a DMPC or DSPC lipid concentration above 500 μg/mL. Breast cancer cells were incubated with liposomes for 48 h (37℃, 5% CO_2). Untreated cells and drug-free liposomes were both used as negative controls.

2.4.2. Cell viability

Cell viability was determined by measuring cellular mitochondrial metabolic activity using the MTT assay (Thiazolyl Blue Tetrazolium Bromide; M2128, Sigma-Aldrich, UK). Briefly, cell culture media was removed from each well, cells were gently rinsed with 1 × PBS and then 150 μL of fresh medium and 30 μL of MTT solution (0.65 mg/mL final concentration in ultrapure water) were gently pipetted to each well. Cells were incubated for 4 h (37℃, 5% CO_2), allowing formazan crystal formation. After 4 h, cell culture media was removed from each well and replaced with 200 μL of DMSO; the plate was gently agitated for 5 min at RT to dissolve the formazan crystals. Absorbance was measured at 540 nm using a plate reader (Synergy2 Biotek plate reader, Gen5 software). Experiments were performed in triplicates for each concentration, with biological duplicates ($n = 3$, $N = 2$). IC_{50} values were calculated with GraphPad Prism (Version 7.04) using the [non-linear regression, normalized response–variable slope] model, normalizing value to the control (i.e., untreated cells).

2.5. Statistical analysis

For each experiment the standard deviation (SD) or standard error of the mean (SEM) were calculated. All data points on graphs represent the mean of at least three ($n = 3$) independent experiments ± SD, unless otherwise stated. One-way analysis of variance (ANOVA) was performed using GraphPad Prism 7.04, as to analyze the significant differences among results. Probabilities were set at four different significance levels: $p < 0.05$ (*$p \leq 0.05$, **$p \leq 0.01$, ***$p \leq 0.001$, ****$p \leq 0.0001$).

3. Results and discussion

3.1. Effects of microfluidic processing parameters on drug-free liposomes

Following the results obtained in our previous work (Gkionis et al., 2020), optimised manufacturing parameters were used for the preparation of liposomes using the microfluidic system. Specifically, the lipid concentration feed in the organic phase was kept at a concentration of 10 ± 2 mg/mL per formulation. $DSPC_{100}$ liposomes were prepared with the FRR constant at 1:10 and the TFR set at 500 μL/min. For the newly prepared $DMPC_{100}$ liposomes, fabrication was monitored with a constant FRR at 1:10, while varying the TFR of both the organic and aqueous phases between 250 and 750 μL/min.

The dynamic viscosity of the $DMPC_{100}$ and $DSPC_{100}$ organic phases was measured, and similar values at 25℃ and 40℃ were reported (Table 2). This further confirmed that similar manufacturing parameters could be used for the fabrication of liposomes using the microfluidic system.

The impact of TFR on $DMPC_{100}$ and $DSPC_{100}$ liposomes Z-average size and PDI is reported in Fig. 1. In particular, the sizes of $DMPC_{100}$ liposomes obtained from a lipid feed 10 mg/mL (Fig. 1**A**), had the lowest

Table 2
Dynamic viscosity values (mPa·s) of organic phases ($DMPC_{100}$ and $DSPC_{100}$ lipid solutions) and aqueous phase (water). Values were measured at 25℃ and 40℃, and data are presented as mean ± st.dev. of $n = 3$ independent samples. The dynamic viscosity of water and HEPES buffer were assumed to be similar in the temperature range of interest, with measured values at 20 °C, being reported to be 1.0016 mPa·s and 1.0104 mPa·s for water and HEPES buffer, respectively (Chairatana et al., 2016).

Temperature	Organic phase $DMPC_{100}$	$DSPC_{100}$	Aqueous phase H_2O
25℃	0.602 ± 0.010	0.601 ± 0.002	0.889 ± 0.001
40℃	0.471 ± 0.002	0.415 ± 0.005	0.554 ± 0.001

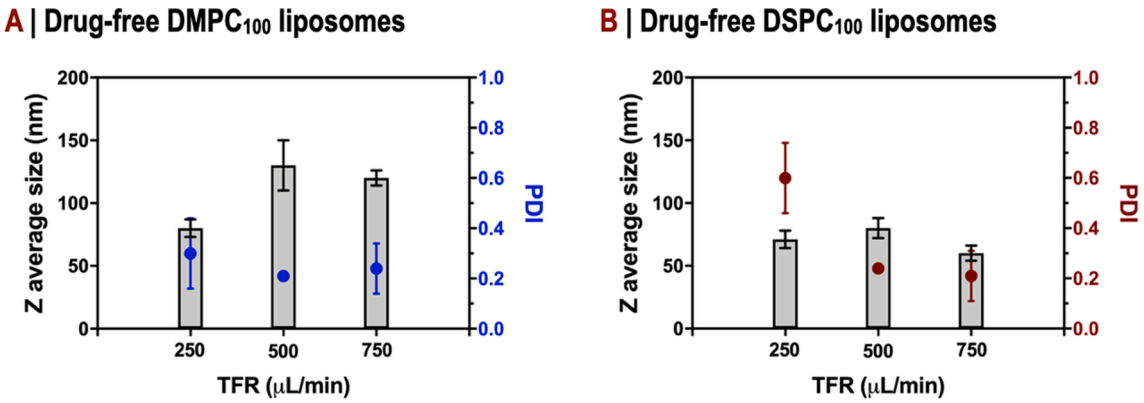

Fig. 1. Optimization steps for the fabrication of drug-free liposomes using the microfluidic Dolomite system. HEPES solution was used as the aqueous phase, and the FRR was set to 1:10, based on results from our previous work. Drug-free liposome size was measured using DLS and reported as Z-average size and PDI. The effect of TFR on liposome size during fabrication is reported for: **A**) $DMPC_{100}$ liposomes and **B**) $DSPC_{100}$ liposomes. Data are presented as mean ± st.dev, (n = 3 independent liposomal formulations, N = 3 measurements for each sample).

PDI value (0.20) and Z-average size of 137.0 ± 9.0 nm at TFR 500 μL/min. By increasing the TFR to 750 μL/min, slightly smaller liposomes with PDI of 0.24 were obtained. Notably, at lower TFR values (250 μL/min), a broader size distribution of liposomes was obtained (PDI ≥ 0.3), with an overall smaller Z-average size reported. Independently of the lipid concentration feed used, this finding agrees with our previous report, in which the optimal TFR value for the fabrication of small, unilamellar $DSPC_{100}$ liposomes with average size of 80 nm and PDI values ≤ 0.25, was found to be 500 μL/min (Fig. 1**B**). Of note, a heterogeneous size distribution was only observed for $DSPC_{100}$ liposomes with a lipid concentration feed of ≥ 10 mg/mL; this formulation required a filtration step prior to further use (Gkionis et al., 2020).

$DMPC_{100}$ liposomes size and size distribution were also confirmed by image analysis using TEM acquisitions (Fig. 2). The morphology of $DMPC_{100}$ liposomes fabricated using different TFR values were compared, with the most homogeneous liposomes in both size and shape observed with TFR of 500 μL/min (Fig. 2**B**). At a lower processing speed (250 μL/min), two distinct liposomal populations were observed with size of approx. 40 nm and 160 nm (Fig. 2**A**), which was not detected by DLS. With a TFR of 750 μL/min, the presence of a smaller population of liposomes with size ≤ 50 nm was also detected (Fig. 2**C**).

Both DLS and TEM analysis confirmed that by using TFR of 500 μL/min, FRR 1:10 and 40℃ or 60℃ working temperature, small, unilamellar liposomes were obtained for both $DMPC_{100}$ and $DSPC_{100}$ liposomes. Interestingly, agglomeration was not observed in $DMPC_{100}$ liposomes.

3.2. Physicochemical characterization of doxorubicin-loaded liposomes

3.2.1. Dynamic light scattering: Size and size distribution

Size and size distribution of different liposomal formulations produced with the selected manufacturing parameters (i.e., TFR 500 μL/min, FRR 0.1, lipid feed 10 mg/mL and temperature of 40℃ or 60℃) and using 250 mM ammonium sulphate buffer (aqueous phase) were firstly evaluated by DLS. There are several factors that may influence the Z-average diameter of liposomes fabricated using microfluidics; typically these are the phospholipids (charge, saturation degree, polar head area, transition temperature) used, the lipid mixture concentration, the mixing temperature, the chip architecture and the flow parameters of the system (Kastner et al., 2015; Capretto et al., 2013). In this study, HEPES buffered saline was used as continuous phase for the production of drug-free liposomes, whereas the protocol of active loading by Haran et al. [26]was used for the encapsulation of doxorubicin hydrochloride, using 250 mM ammonium sulphate buffer as aqueous phase.

Using the optimised manufacturing parameters previously described, drug-free $DMPC_{100}$ liposomes were prepared with a Z-average size of 136 nm (unfiltered) and PDI 0.21, whereas larger drug-free $DSPC_{100}$ liposomes were prepared (235 nm; post-filtered) with a similar size distribution profile (PDI 0.23). Results of Z-average size and PDI of

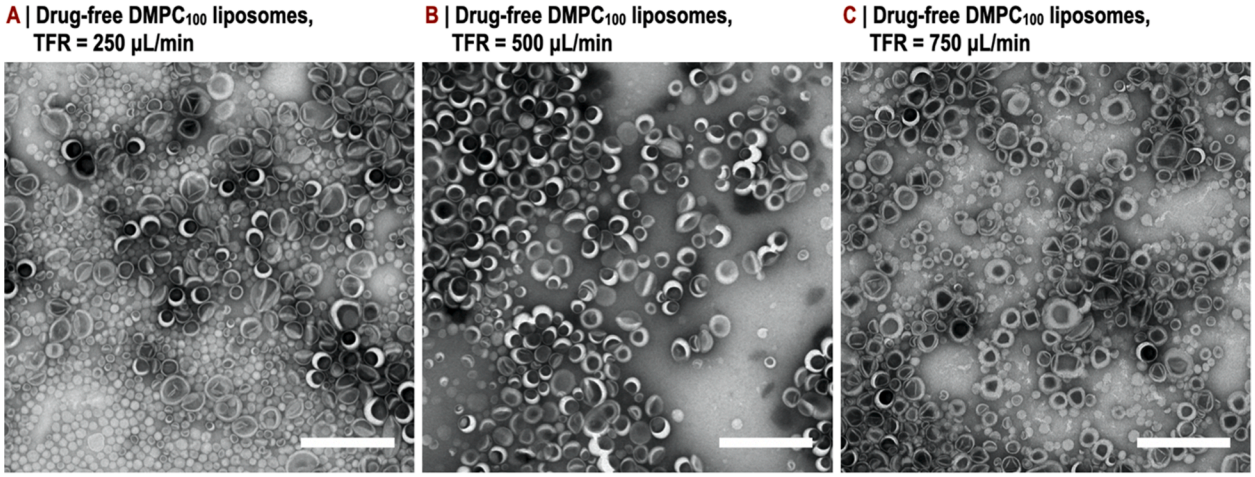

Fig. 2. TEM images of drug-free $DMPC_{100}$ liposomes. Morphological analysis of liposomes preprared using microfluidics to assess the effect of total flow rate (TFR): **A**) 250 μL/min, **B**) 500 μL/min and **C**) 750 μL/min. Flow rate ratio (FRR) was set to 1:10 for all sample preparations, with controlled temperature of 40℃. All images were acquired at 6800X; Scale bars 500 nm.

liposomes containing ammonium sulphate are reported in Table 3.

After doxorubicin encapsulation, the drug-loaded $DMPC_{100}$ liposomes exhibited a Z-average size and size distribution profile similar to their drug-free counterparts (Table 4), with no significant variations observed ($p > 0.05$, NSD; one-way ANOVA). On the contrary, $DSPC_{100}$ doxorubicin-loaded liposomes increased in size by approximately 15% (273.0 ± 2.1 nm) with a simultaneous reduction of PDI (0.13 ± 0.03). Results were found statistically different when compared to the drug-free samples ($p = 0.0046^{**}$ (≤ 0.01), one-way ANOVA).

The Z-average sizes of the doxorubicin-loaded liposomes fabricated using different DSPC/DMPC ratios ($DMPC_{0.2}$ – $DMPC_{10}$) were all in the range of 80–110 nm and had PDI values within 0.13–0.16 (Table 4). As expected, the ξ -potential of all liposomal formulations was slightly negative, since the lipids used in this study were all zwitterionic, regardless of the loading of doxorubicin.

Size stability of the doxorubicin-loaded liposomes was measured by DLS after 2 weeks storage at 4 °C (Table 4). No significant differences were observed both in Z-average size or PDI ($p > 0.05$, NSD; one-way ANOVA).

To better compare liposome size and size distribution, we present in detail a full of summary of the different size distributions obtained from DLS (Table 5). Intensity weighted distribution results from the first order transformation of the scattering intensity of spherical particle fractions or distinct populations (Pecora, 2000; Carvalho et al., 2018). This scattering intensity is proportional to the square of the molecular weight. Applying the Mie theory, the intensity-weighted distribution can easily generate the mode of volume-weighted distribution, which represents the relative proportion of volume occupied by differently sized particles in a particular sample (Stetefeld et al., 2016). Instead, the volume distribution relies on the main assumption that all particles are spherical in shape, homogenous and with known optical properties, namely the real and imaginary components of the refractive index. Considering the Rayleigh approximation, the mass of spherical colloidal particles is proportional to their d^3 (diameter). The mass can therefore be approximated to volume, if the system's density is uniform. As a consequence, the volume-weighted distribution is proportional to d^3 and it bears hydrodynamic radius (R_h) smaller to that of intensity-weighted distribution (Stetefeld et al., 2016). According to DLS manufacturers, it is usually preferable to report the size of the peak based on an intensity analysis and report the relative percentages only (not size) from a volume distribution analysis. The importance of sharing this information is associated appropriately at **Section 3.2.3** below.

3.2.2. *Effect of lipid composition on liposome thermotropic behavior*

Doxorubicin-loaded $DMPC_{100}$ liposomes exhibited a main pre-transition temperature of 40.3 ± 1.4℃ (n = 3 independent samples), while their main phase transition (T_g) increased up to 59℃, as shown both in Table 4 and the DSC thermograph in Fig. 3. Herein, we defined pre-transition as the transformation from a tilted to a rippled chain gel phase ($L_{\beta'} \rightarrow P_{\beta'}$), and the main T_g as the transformation from the gel to the liquid crystalline phase ($P_{\beta'} \rightarrow L_\alpha$) (Ali et al., 2000). Typical T_g values of DMPC liposomes above 25℃ are reported in literature with cholesterol contents > 25% mol (Trandum et al., 2000; Needham et al., 1988; Mcmullen and Mcelhaney, 1995). Cholesterol species usually separate the system to a cholesterol rich liquid ordered phase (*lo*) (i.e. high degree of alkyl chain order) and a cholesterol poor phase at an equilibrium (Corvera et al., 1992; Redondo-Morata et al., 2012). These two phases are in equilibrium with each other until the overall cholesterol concentration of the mixture reaches that of the *lo* phase, around at 30 mol %. At higher cholesterol contents (>30% mol), an enrichment of the fluid phase in solubilised cholesterol occurs (Redondo-Morata et al., 2012), with the lipid chains to be characterized by a high degree of conformational and positional order (Trandum et al., 2000). Additionally, the presence of DSPE-PEG2000-PE lipid accounts for this upward shift (Turjeman, 2015).

On the contrary, doxorubicin-loaded $DSPC_{100}$ liposomes in the presence of both 30% mol cholesterol and encapsulated amphipathic doxorubicin, presented a slight shift reduction with respect to their overall thermotropic behaviour, with a pre-transition occurring at 49℃ (attributed to cholesterol poor region of the bilayer) and a second main and broader endothermic component corresponded to the cholesterol rich or liquid-ordered melting point at around 55-56℃.

Moreover, the phase transition enthalpy (ΔH) of the doxorubicin-loaded $DMPC_{100}$ formulations was at 4.17 J/g, whereas it was at 3.58 J/g (i.e., weaker lipid chain-chain associations; ΔH data not shown) for the $DSPC_{100}$ liposomes. A decrease in ΔH suggests perturbation in the bilayer region, which is usually associated with disassociation of the intermolecular forces between the lipophilic acyl chains, and hydrogen bond disruption at the polar head-water interface (Turjeman, 2015; Ali et al., 2000). Interaction of neutral doxorubicin species with either DPPC (Mady et al., 2012) or DMPC (Alves, 2017) model membranes, upon translocation to the interfacial region of the bilayer, has been found to reduce the plastic microviscosity of the lipid membrane in its liquid-disordered regions, while enhancing the membrane fluidity of the gel-type regions. This result demonstrates the importance of the drug-lipid interactions, as well as the influence of the presence of cholesterol in the lipid bilayer. The presence of drug molecules and cholesterol species – either in the intraliposomal compartment or within the lipid bilayer – rearranges the van der Waals forces among the acyl lipid chains and the interactions among the polar heads (Montenegro et al., 2018; Fonseca et al., 1997).

The glass transition temperature of the doxorubicin-loaded DSPC/DMPC mixed liposomes exhibited values between 25 and 55℃ as theoretically expected (DSC thermographs shown in Fig. 3). Specifically, the $DMPC_5$ and $DMPC_3$ mixtures exhibited the highest pre-transition values of approx. 44.0 ± 1.0℃, followed by the $DMPC_{10}$ and $DMPC_{0.2}$ mixtures at 40.0 ± 1.0℃. The main phase transition from gel to liquid crystalline phase for both $DMPC_5$ and $DMPC_3$ vesicles occurred at 51℃, whereas for $DMPC_{10}$ and $DMPC_{0.2}$ it occurred at nearly 44℃ (Table 4). The latter formulations demonstrated rather broad and poorly resolved endotherms without sharp melting peaks upon temperature increase. It could be hypothesised that both binary samples favoured the disordered L_β gel phase rather than the crystalline sub-gel L_c one. The results obtained are in accordance with the reported data of Losada-Pereze et al. (Losada-Pérez, 2015) for $DMPC_{0.2}$ drug-free liposomes (a non-ideal formulation). $DMPC_5$ and $DMPC_3$ liposomes can be considered the more stable formulations (phase transition enthalpies at 5.5 ± 0.6 J/g and glass transition temperatures > 50℃), as compared to the rest of the PC mixed formulations composed predominantly of either DSPC (i.e., $DMPC_{0.2}$) or DMPC (i.e., $DMPC_{10}$). The latter formulations exhibited considerably lower transition enthalpies (ΔH at 0.45 ± 0.28 J/g), an approx. 12-fold diminution over the molecular interaction strength.

Over the past decades, the (1:1) DSPC/DMPC mixed model bilayers have been thoroughly investigated for their complex thermodynamic and structural properties (Koynova and Caffrey, 1998; Michonova-Alexova and Istvan, 2002). Pokorny et al. (Pokorny et al., 2001) have reported that in DMPC liposomes, gel (*s*) and highly disordered liquid (l_d) phases coexist at the melting temperature (T_m), whereas in a (1:1) DSPC/DMPC mixture a stable ($s + l_d$) phase separation of a non-ideal mixture is observed over a large temperature interval of approx. 28-55℃ (Fig. 7). A phase diagram of this binary system indicates a peritectic behaviour at the aforementioned temperature zone (because of the lipid's T_g difference gap) (Knoll et al., 1981; Pokorny et al., 2001), with a

Table 3
Z-average size and PDI of drug-free liposomes containing ammonium sulphate solution. Data are presented as mean ± st.dev. of n = 3 independent formulations; each result is the mean of N = 3 measurements.

Liposomes	ξ-average size (nm)	PDI	ξ -potential (mV)
$DMPC_{100}$	136.0 ± 7.3	0.21 ± 0.04	– 0.7 ± 0.5
$DSPC_{100}$	235.0 ± 11.3	0.23 ± 0.02	– 2.8 ± 0.4

Table 4
Physicochemical characteristics of doxorubicin-loaded liposomal formulations after preparation and storage (2 weeks, 4℃). Doxorubicin was actively loaded into liposomes after manufacturing, with ammonium sulphate buffer used as the continuous phase, in the microfluidic system. Of note, samples were not filtered after production and prior to measurements, except for the $DSPC_{100}$ liposomes. Data are presented as mean ± st.dev. of n = 3 independent formulations, each result is the mean of N = 3 measurements.

Liposomes	ξ-average size (nm)		PDI		ξ -potential (mV)	Pre-transition phase (℃)
	As prepared	After storage	As prepared	After storage	As prepared	As prepared
$DMPC_{100}$	143.0 ± 6.4	148.0 ± 0.2	0.22 ± 0.02	0.21 ± 0.01	− 0.3 ± 0.4	40.3 ± 1.4
$DMPC_{10}$	82.0 ± 2.0	95.0 ± 1.0	0.13 ± 0.01	0.23 ± 0.01	−2.1 ± 0.9	44.6 ± 0.5
$DMPC_5$	104.0 ± 0.4	110.0 ± 0.2	0.14 ± 0.01	0.18 ± 0.01	−2.0 ± 0.4	51.1 ± 1.2
$DMPC_3$	84.0 ± 0.2	91.0 ± 0.4	0.14 ± 0.01	0.20 ± 0.01	−2.6 ± 0.2	51.3 ± 0.9
$DMPC_{0.2}$	110.0 ± 1.0	125.0 ± 1.8	0.16 ± 0.01	0.15 ± 0.02	−1.6 ± 0.7	44.5 ± 2.3
$DSPC_{100}$	266.0 ± 1.42	273.0 ± 2.1	0.22 ± 0.01	0.13 ± 0.03	− 2.0 ± 0.2	48.9 ± 0.3

Table 5
Size analysis of mixed phosphatidylcholine liposomes prepared by microfluidics. Data are reported for doxorubicin-loaded liposomes. With the exception of $DSPC_{100}$ liposomes, all samples were not filtered after fabrication and prior measurements. Data are presented as mean ± st.dev. of n = 3 independent formulations, each result is the mean of N = 3 measurements.

Liposomes	Dynamic Light Scattering analysis			
	Z-average size (nm)	PDI	% Intensity Size (nm)	% Volume Size (nm)
$DMPC_{100}$	143.0 ± 6.4	0.22 ± 0.02	(100%)	(100%)
			164.0 ± 8.7	102.0 ± 0.2
$DMPC_{10}$	82.0 ± 2.0	0.13 ± 0.01	(100%)	(100%)
			95.0 ± 2.7	68.0 ± 1.9
$DMPC_5$	104.0 ± 0.4	0.14 ± 0.01	(100%)	(100%)
			123.0 ± 0.5	86.0 ± 2.6
$DMPC_3$	84.0 ± 0.2	0.14 ± 0.01	(100%)	(100%)
			94.0 ± 0.5	70.0 ± 1.3
$DSPC_{100}$	266.0 ± 1.42	0.22 ± 0.01	(100%)	(100%)
			322.0 ± 18.4	351.0 ± 33.0

broad horizontal solidus line up to at least 60% mol DSPC content (Nicolussi et al., 1982). In our study, the maximum DSPC ratio obtained was 57% – with the $DMPC_{0.2}$ formulation. The rest of the samples contained<20% mol DSPC in their overall composition. Thermographs obtained by Matubayasit and co-workers showed that pure DSPC/DMPC lipid mixtures form mixed crystalline phases at temperatures below the solidus curves of the main transition point (i.e. 28℃) (Matubayasit et al., 1986). At a given temperature, if some of the components are in a liquid state and the rest are in the gel state, these two phases can coexist in spatially separated populations. At low temperatures (i.e. < 20℃) the binary system crystallises separately upon cooling and therefore lateral phase separation occurs in the gel state (Matubayasit et al., 1986). In general, DSPC/DMPC binary mixtures behave non ideally in the solid state, especially for a DSPC molar content between 50 and 60% (Nicolussi et al., 1982), and this was evidenced in our results as well.

3.2.3. *Microscopic analysis: Morphology and size (TEM)*

Transmission Electron Microscopy was used to assess the morphology, as well as size and size distribution of doxorubicin-loaded liposomes. The analysis confirmed that spherical, small unilamellar vesicles (SUVs) were obtained for all liposomes tested, as evidenced in Fig. 4 and Fig. 5. With the exception of $DSPC_{100}$, all liposomes exhibited sizes < 200 nm after fabrication, without any post-modification steps (e.g., filtering, sonication or extrusion). This result is important for the use of liposomes in drug delivery applications, as meeting the size criteria of 50–150 nm for efficient accumulation in the targeted tumour mass (Kraft et al., 2014).

More specifically, drug-free $DMPC_{100}$ liposomes exhibited a higher degree of homogeneity/uniformity of size and size distribution when compared to doxorubicin-loaded liposomes (Fig. 4**A**), and in accordance with DLS measurements (Table 3, Fig. 1). After loading with doxorubicin, a reduction in liposome size was observed, with diameters in the range of 50–90 nm (Fig. 4**B**). A similar behavior, with a reduction in size of doxorubicin-loaded liposomes, was observed in all the other drug-loaded liposomes (Fig. 5).

Liposomes' average size measured by TEM (Fig. 4, Fig. 5), is similar

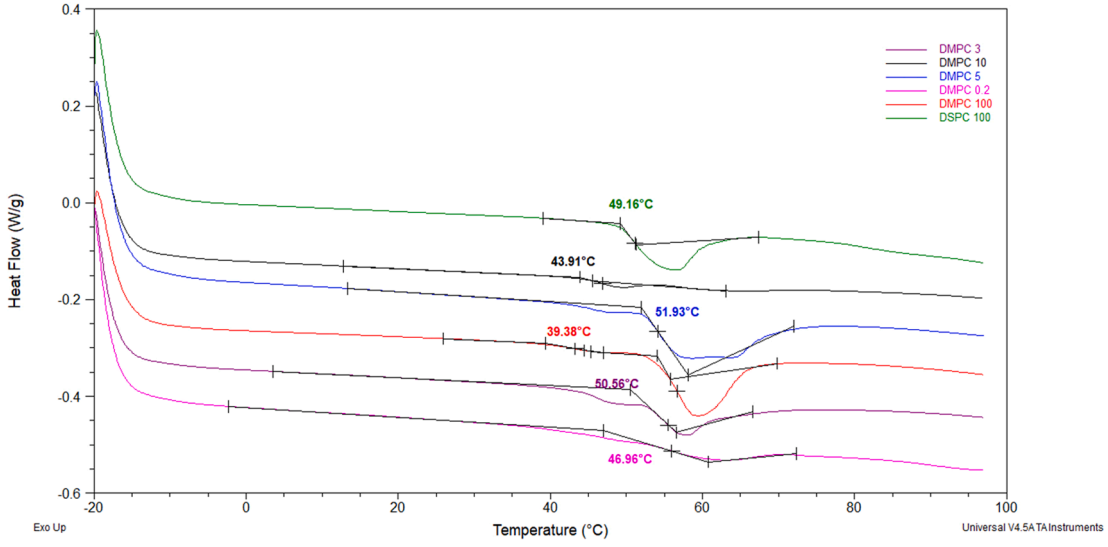

Fig. 3. DSC thermographs (Heating flow (W/g)/ Temperature (℃)) of doxorubicin-loaded liposomes with different DSPC/DMPC lipid ratio prepared using the Dolomite microfluidics system. The samples were scanned in the range of −20 − 100℃, at a heating rate of 5℃/min. Representative plots of n = 3 independent preparations.

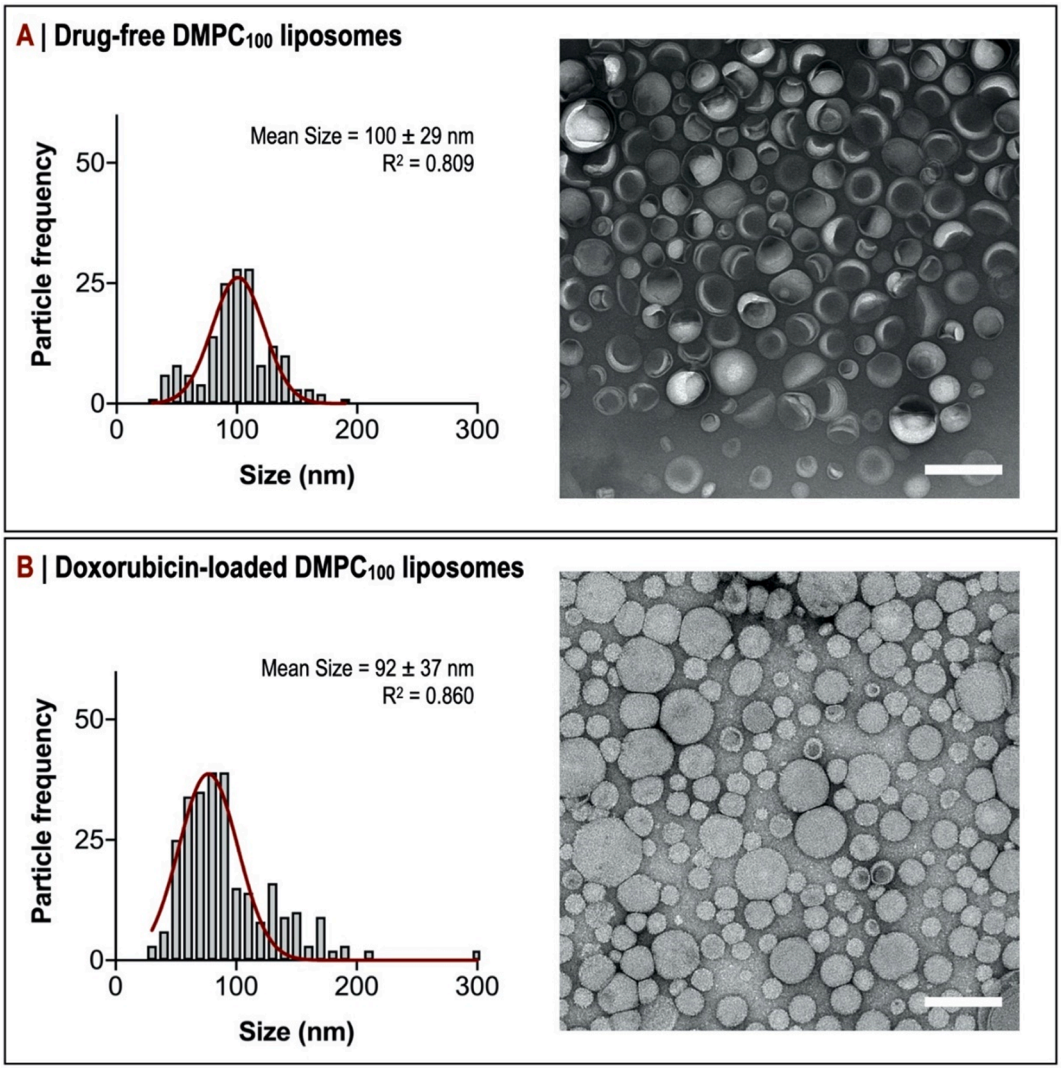

Fig. 4. TEM analysis. Morphology and size distribution of: (**A**) drug-free and (**B**) doxorubicin-loaded $DMPC_{100}$ liposomal formulations. Mean size and size distribution of liposomes from TEM images was obtained by fitting N > 200 liposomes (n = 3 images) and was similar to the Z-average size and PDI values measured by DLS (Table 3). Particle size frequency distribution (mean size ± st.dev.) and Gaussian fitting (R^2 values) were obtained using GraphPad Prism. Scale bars: 200 nm.

to the % volume size distribution data obtained from DLS (Table 5), with a mean size in the range of 70–90 nm. This observation suggests that the % volume size distribution is more precise than the % intensity size distribution or the Z-average size, when it comes to measure the 'actual' size of phosphatidylcholine liposomes.

As shown in Fig. 5, all liposomes presented a homogeneous population of vesicles (only exception $DSPC_{100}$ liposomes). Fitting of $DMPC_3$ liposome size reported a mean size of 70 nm (Fig. 5**A**, Gaussian fit $R^2 > 0.95$). $DMPC_5$ liposomes were slightly more heterogeneous, with spherical vesicles of 90 nm in average and a second population of vesicles ranging 50–60 nm (Fig. 5**B**, Gaussian fit $R^2 = 0.77$). $DMPC_{10}$ liposomes presented also a mild heterogeneity with a mean size of 76 nm (Fig. 5**C**, Gaussian fit $R^2 = 0.83$). With the slight exception of the $DMPC_5$ formulation, the measured TEM diameter of the other two formulations was highly consistent with respect to both the Z-average and % volume distribution sizes (Table 5, DLS).

Notably, TEM and DLS results reported different sizes of $DSPC_{100}$ liposomes, with a larger Z-average size (approx. 270 nm, DLS) of hydrated liposomes against the average size of 110 nm (TEM) of dry liposomes. Of note, this was the only sample filtered through 0.22 μm PVDF filters after fabrication, due to the heterogeneity/agglomeration phenomena previously observed (Gkionis et al., 2020). Image analysis (TEM) revealed only few LUVs with size > 250 nm, which is not in accordance with DLS data. The shape of the $DSPC_{100}$ liposomes was more irregular than all the other liposomes presented in this study: a large proportion of vesicles displayed an asymmetrical shape, with one dimension above 200 nm; this may impact on the DLS measurements.

Overall, it is possible to conclude that both analysis methods used (DLS, TEM), returned a similar of liposomes' size with $DSPC_{100} \gg DMPC_{100} > DMPC_5 > DMPC_3 \geq DMPC_{10}$ (DLS method) and $DSPC_{100} > DMPC_{100} > DMPC_{10} > DMPC_5 > DMPC_3$ (TEM method).

3.2.4. *Influence of lipid composition on drug loading and release kinetics*

Doxorubicin encapsulation efficiency (EE%) was found higher than 80% in both $DMPC_{100}$ and $DSPC_{100}$ formulations (Table 6). Drug Loading % levels exceeded the 30% overall drug content value considered acceptable for intratumoral delivery of potent chemotherapeutic agents like doxorubicin or paclitaxel (Rocca et al., 2012). Among the different PC mixed-liposomes presented in this study, $DMPC_{10}$ and $DMPC_{0.2}$ (which had a higher % mol content of either DMPC or DSPC lipid) showed the highest concentration of loaded doxorubicin, with an encapsulation efficiency of 88% for $DMPC_{10}$ liposomes and 70% for $DMPC_{0.2}$ liposomes (***Supplementary Information, SI.1 Table***). The two intermediate formulations, $DMPC_5$ and $DMPC_3$, both exhibited lower

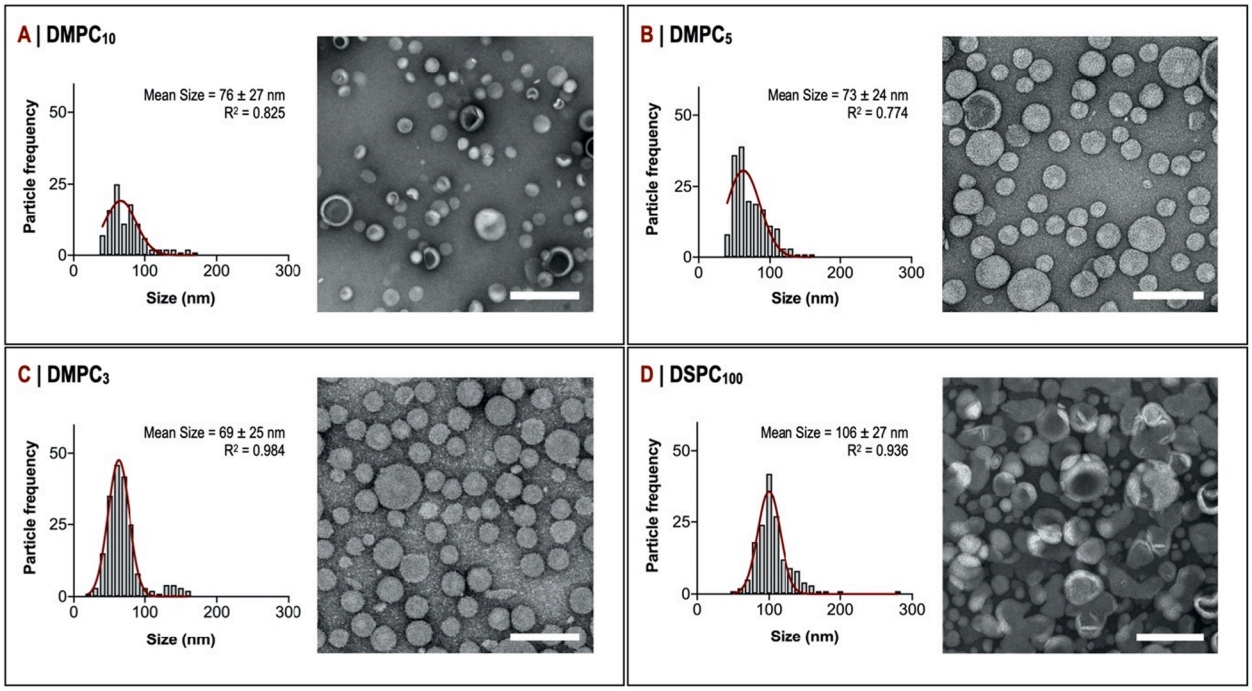

Fig. 5. TEM analysis. Morphology and size distribution of doxorubicin-loaded: (**A**) $DMPC_{10}$, (**B**) $DMPC_5$, (**C**) $DMPC_3$ and (**D**) $DSPC_{100}$ PC liposomes. Mean size and size distribution of liposomes from TEM images was obtained by fitting N > 200 liposomes (n = 3 images) and was similar to the Z-average size and PDI values measured by DLS (Table 3). Particle size frequency distribution (mean size ± st.dev.) and Gaussian fitting (R^2 values) were obtained using GraphPad Prism. Scale bars: 200 nm.

Table 6
Encapsulation efficiency (%EE) and drug loading (%DL) levels of doxorubicin in phosphatidylcholine-mixed liposomes prepared by the Dolomite microfluidic system. Doxorubicin feed was set to 0.2 mg/mL for all microfluidic samples; active loading. Data are presented as mean ± st.dev. of n = 3 independent formulations, N = 3 measurements each.

Liposomes	EE (%)	DL (%)
$DMPC_{100}$	84.0 ± 5.3	30.0 ± 5.2
$DMPC_5$	59.0 ± 12.3	17.0 ± 11.1
$DMPC_3$	58.0 ± 12.4	15.0 ± 0.3
$DSPC_{100}$	89.4 ± 0.2	37.0 ± 0.1

ability to encapsulate doxorubicin, with EE% of 59 ± 12% and DL% < 20%.

It has been recently reported that when short in length hydrocarbon chains (e.g. 12:0 PC-14:0 PC lipids) are included in liposomal formulations, reduced drug encapsulation efficiency and faster drug release are observed (Anderson and Omri, 2004; Ali et al., 2013). Whereas, when phospholipids with long acyl chains are included in the lipid bilayer, a higher drug loading capacity is observed. This could be attributed to an increased bilayer spatial area formed by the longer lipid chains. In this configuration, it has been hypothesized that the loaded drug has a slower release profile due to a wider physical barrier through which the drug has to diffuse (Dan, 2007). Our findings are in accordance with those reported by Ann et al., with comparable drug encapsulation efficiencies of doxorubicin (using a pH-gradient encapsulation protocol) observed with both phospholipid types used, and regardless of the acyl chain length (Ann et al., 1565).

The liposomal cholesterol content is known to impact on doxorubicin encapsulation and release (Corvera et al., 1992). In this study, the cholesterol content was kept constant at 30–35% mol in all liposomes, and considered to be an optimal fraction for sustained drug release (Briuglia et al., 2015). The inclusion of cholesterol to the lipid bilayer leads to significant enhancement of doxorubicin transport across the bilayer at temperatures above the T_g threshold (Farzaneh, 2018). Cholesterol is hypothesized to facilitate doxorubicin transition by reducing the hydrophobicity of the bilayer, which is composed of saturated phospholipids with high logP values. DMPC liposomes have been reported to encapsulate slightly less cargo compared to liposomes consisting of longer saturated phospholipids like 16:0 PC-18:0 PC (Farzaneh, 2018).

In this study, both DMPC-rich formulations (i.e. $DMPC_{100}$ and $DMPC_{10}$) were found to have a high EE% (>80%) with a potential influence of cholesterol on this outcome (Fonseca et al., 1997). In fact, the presence of cholesterol in DMPC bilayers reduces the membrane fluidity near the bilayer's surface, whereas increased fluidity has been observed near the bilayer centre (Subczynski et al., 2017); therefore elevated rates of drug transport. Alves et al. have shown specifically that cholesterol can facilitate a drug's accumulation into the cholesterol-rich, liquid-ordered regions of the liposomal bilayer, by strengthening the hydrogen bonding between the drug and the polar heads of both phospholipids and cholesterol species (Alves, 2017). Accordingly, cholesterol could influence the DSPC-rich bilayer rigidity (pre-transition onset – lower than 55-56℃ – was observed at DSC thermographic analysis) and therefore promote doxorubicin diffusion across the bilayer, resulting in increased drug encapsulation (almost 90%) for incubation at temperatures ≥ 60℃.

In the case of a DSPC content lower than 20% mol, liposomes (i.e., $DMPC_3$, $DMPC_5$) are mainly characterised by mixed liquid-crystalline and liquid-fluid phase regions. The cholesterol-modulated impact on the bilayer's rigidity may have contributed to the formation of ordered segregated domains on the planar membrane, as evidenced by rather high T_g levels observed at ~ 51℃ (Soto-Arriaza et al., 2013; Raffy and Teissié, 1999; Soto-Arriaza et al., 2013). This may have resulted in a lower diffusion rate of doxorubicin across the liposomal membrane, which was reflected by lower encapsulation efficiency levels (EE% levels almost 1.3-fold lower). A free-energy mismatch, over the partitioning of the drug to the assorted liquid-ordered and liquid-disordered regions of the binary lipid membrane, could somehow slow or even inhibit the

translocation process.

No further study on membrane rigidity was performed, but further investigations may be required to better understand the intermolecular interactions between cholesterol and DSPC/DMPC phospholipid mixtures containing up to 20% mol DSPC.

Drug release kinetics is a critical parameter used to define the ability of liposomes to deliver a sufficient dose of the payload(s) over time to the pathological areas of interest (Wallace et al., 2012). Many reports have shown that PC lipids with longer fatty acid chains possess larger head-polar groups and stronger lipid-chain cohesion forces, as well as exerting stronger steric effects and undergoing hydrolysis more slowly. In the present study we expected to observe a more sustained drug release with liposomes high in DSPC content and with a predicted release of DSPC≫DPPC > DMPC (Mohammed et al., 2004; Swenson et al., 2001).

However, $DSPC_{100}$ liposomes (upon prior purification) showed a burst release of the loaded doxorubicin, with>85% of the loaded drug being released within the first 48 h (Fig. 7), according to Korsmeyer-Peppas kinetic release model accounted to Fickian diffusion ((logC/C_0 vs logt, where C is the drug amount at t time and C_0 the maximum drug content; linear fitting $R^2 = 0.998$, $n < 0.5$ for sphere shaped delivery matrixes). The main reason for this result could be attributed to the final low lipid concentration of the vesicles (i.e., ≤0.6 mg/mL). Moreover, the drug-to-lipid ratio for an EE% of nearly 90% (corresponding to 0.18 mg dox/mL in suspension) and a final DSPC concentration between 0.4 and 0.6 mg/mL, reaches values up to 1:2.5. This proportion is considered rather high despite the active encapsulation mechanism of doxorubicin. In this setting, it is possible to assume a potential semi-crystallisation of doxorubicin; as a consequence, the vesicles could be unable to retain the entrapped doxorubicin-sulphate salt complex under physiological conditions, resulting in a faster release. In accordance to this observation, it has been reported that unbundled doxorubicin molecules have a 5-fold faster release profile (~60% release in human plasma in first 20 min after injection) compared to their bundled form (only 10% release) (Cohen, 2014).

$DMPC_{100}$ liposomes released up to ~ 45% of the loaded drug within the first 48 h at 37℃ (Fig. 7). These release kinetics corresponded to the first order release model (log percentage of drug release vs time; linear fitting $R^2 = 0.959$, slope −1.24) (Muderhwa et al., 1999). Surprisingly, these liposomes although with a shorter alkyl chain phospholipid (and lower T_g), exhibited a sustained drug release profile compared to the $DSPC_{100}$ vesicles.

Among the DSPC/DMPC mixed liposomes, the formulation with the most prolonged release profile was $DMPC_5$, with maximal release of ~ 38% of the doxorubicin from the liposomes during the 48 h incubation; a rapid release observed over the first 2 h (Fig. 6). The $DMPC_3$ formulation was able to release approximately 60% of encapsulated doxorubicin over 48 h incubation, with almost 30% of the drug to be released after the first 6 h of incubation followed by a gradual increase over time. The kinetics of doxorubicin release corresponded to the first order release model for the $DMPC_3$ formulation (log percentage of drug release vs time; linear fitting $R^2 = 0.975$, slope −0.65), whereas the $DMPC_5$ formulation exhibited zero-order kinetics ((cumulative percentage of drug release vs time; linear fitting $R^2 = 0.902$, slope 0.31). This result could be attributed to the high transition temperature (around 51℃) of the formulation, that is higher than the simulated physiological conditions used in the release studies (37℃). In addition, both the $DMPC_{10}$ and $DMPC_{0.2}$ formulations exhibited a burst release of the drug within the first 6 h of incubation, with almost complete release at 48 h.

Of note, the final phospholipid concentration of $DMPC_{100}$, as well as that of DSPC/DMPC mixed liposomes presented in this study, was between 0.6 and 0.9 mg/mL. This could explain the slower doxorubicin release when compared to $DSPC_{100}$ liposomes. A decrease of the phospholipid concentration could result in significant destabilisation of the bilayer integrity, leading to fusion and aggregation phenomena (Chong, 2004).

The poor capacity to retain doxorubicin in DSPC/DMPC mixed liposomes when compared to $DMPC_{100}$ liposomes could be explained by what was proposed by Pokorny et al. in 2001. In (1:1) DSPC/DMPC mixtures, the ($s + l_d$) coexistence region is characterised by defect-rich regions between 30℃ and 44℃, which could be phase boundaries between solid and liquid domains (Pokorny et al., 2001). Moreover, it was suggested that the relative amounts of solid and liquid phases are similar at 34℃ (~65% of (s) solid phase is present). As a result, fast association kinetics of solutes were observed in their study, as regards the insertion of amphiphile molecules into the formed DSPC/DMPC LUVs. However, when cholesterol was incorporated in the bilayer resulting in a solid–liquid phospholipids/cholesterol mixture ($s + l_o$), the rate of amphiphile insertion was severely decelerated (Pokorny et al., 2001). The inclusion of cholesterol in the PC mixture should increase the proportion of solid-like phases within the bilayer, with different transition states at physiological temperatures (Pokorny et al., 2001).

As a consequence, the significantly prolonged release of doxorubicin in $DMPC_3$ and $DMPC_5$ liposomes could be attributed to three leading

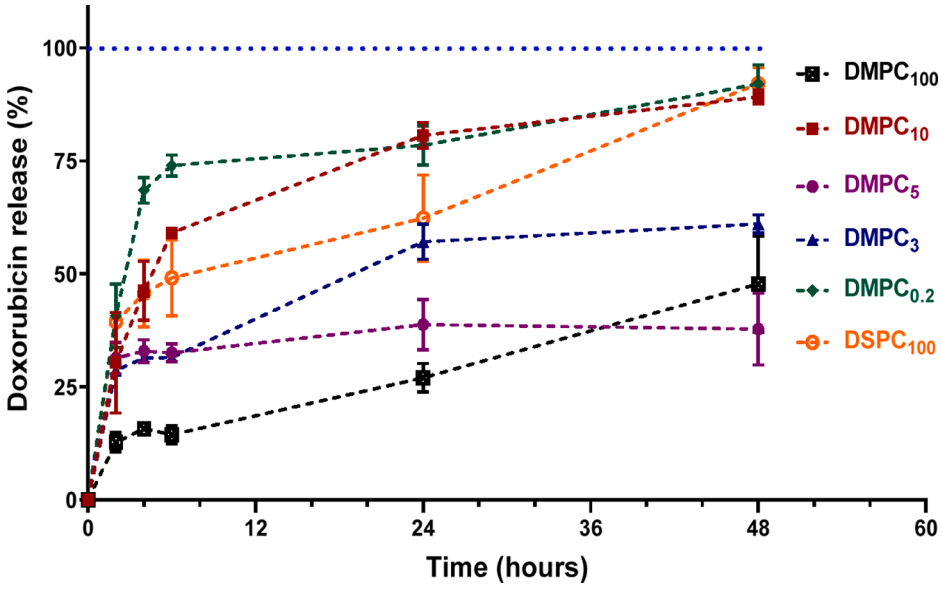

Fig. 6. Doxorubicin release studies. Doxorubicin-loaded DSPC/DMPC mixed liposomes were dialyzed under simulated physiological conditions (1x PBS, pH 7.4, 37℃, 48 h). Samples were taken at different time intervals and analyzed by RP-HPLC. $DMPC_{100}$ (black square, black dotted line), $DMPC_{10}$ (red square, red dotted line); $DMPC_5$ (purple dot, purple dotted line); $DMPC_3$ (blue triangle, blue dotted line), $DMPC_{0.2}$ (green rhombus, green dotted line) and $DSPC_{100}$ (orange dot, orange dotted line). Data are plotted as mean ± st.dev. of n = 3 independent samples for each preparation; The blue dashed line represents 100% released doxorubicin.

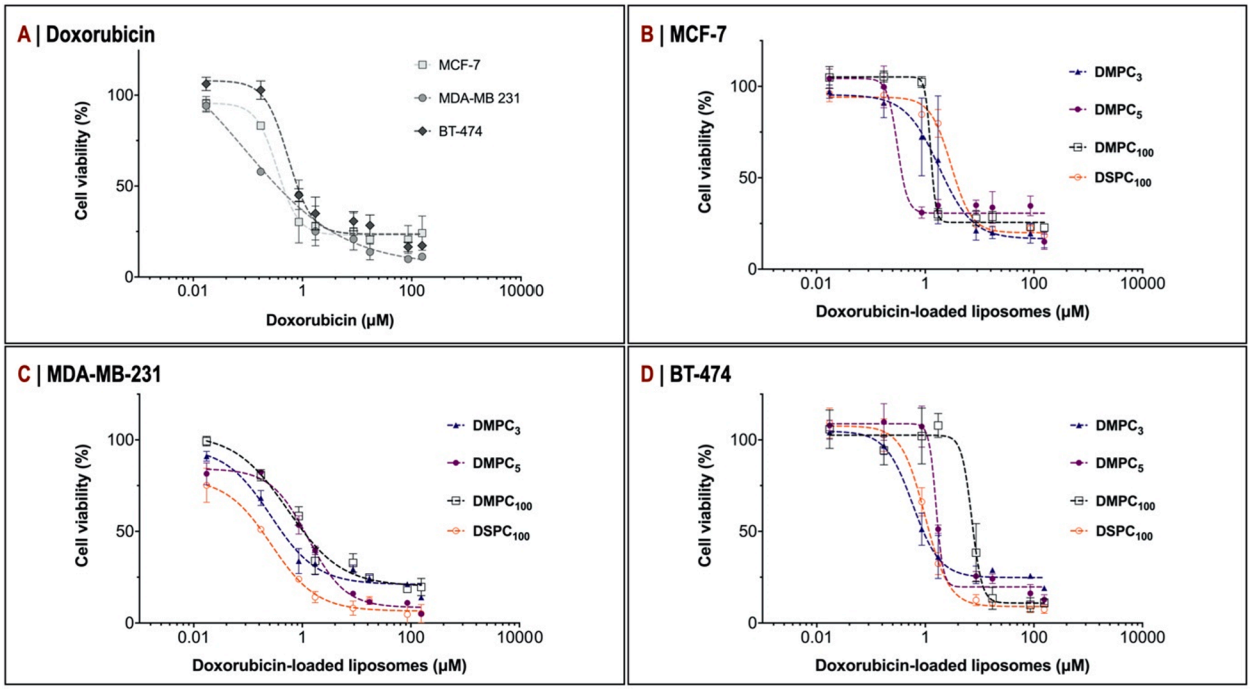

Fig. 7. Cellular mitochondrial metabolic activity (measured by MTT assay) of human breast cancer cells (MCF-7, MDA-MB 231 and BT-474). **A**) Cell viability after 48 h incubation with free doxorubicin in cell culture media (0–155 μM); **B**) MCF-7 cell viability after 48 h incubation with selected doxorubicin-encapsulated mixed phosphatidylcholine liposomes (0–155 μM doxorubicin); **C**) MDA-MB-231 cell viability after 48 h incubation with selected doxorubicin-encapsulated mixed phosphatidylcholine liposomes (0–155 μM doxorubicin); **D**) BT-474 cell viability after 48 h incubation with selected doxorubicin-encapsulated mixed phosphatidylcholine liposomes (0–155 μM doxorubicin). Cell viability was calculated as a percentage of the untreated controls, and each point represents the mean of three independent experiments and data are expressed as mean ± st.dev.

factors:

1) The presence of cholesterol could stabilize/equilibrate the separately distributed gel-liquid phase regions within the bilayer, sealing any inconsistencies at the interfaces. Soto-Arriaza et al. have reported that at 33.3 mol% of cholesterol content, the proportion of the ordered domains in DSPC/DMPC mixtures reached a maximum, even when bilayers heated at 37.5℃ (Soto-Arriaza et al., 2013). At this ratio, the membrane defects or membrane-free volumes are significantly minimised (Soto-Arriaza et al., 2013; Lasic, 1995). In agreement with this, Subczynski et al. have reported the formation of a complete liquid-ordered (l_o) phase in a DMPC/Chol bilayer consisting of ~ 30–50 mol% cholesterol content (Subczynski et al., 2017).
2) Partial crystallization of the actively loaded doxorubicin and physical intermolecular interactions govern its diffusional behaviour across PC:Chol bilayers. A lower drug-to-lipid ratio (up to 1:6 in this case) possibly facilitates complete precipitation/crystallization of the drug-counterion salt, $DOX_2(SO_4)$. The low solubility of $DOX_2(SO_4)$ salt (<2 mM) minimises the intraliposomal osmotic pressure and as such preserves vesicle integrity (Santos, 2004). Additionally, at low intraliposomal pH>90% of doxorubicin species are in the protonated form (Alves, 2017). Either cationic or neutral doxorubicin is found to have a low phospholipid/water partition coefficient (K_p) when transported through cholesterol-containing PC bilayers (Gallois et al., 1996; Modi and Anderson, 2013), particularly in the case of longer acyl chains. A low membrane partitioning, associated with minimal intravesicular membrane binding, reduces significantly the intrinsic rate constant of the drug (Allen et al., 2002).
3) Steric stabilisation of PEGylated liposomes (Viitala and Saija Pajari, 2019). PEGylation increases the phase transition temperature of spherical vesicles, with an increased bilayer thickness and an improved shielding that could change the surface pressure of the bilayer (Rissanen, 2014). Furthermore, PEG imparts repulsive 'protective' forces on the entrapped drug molecules, by creating a physical barrier between the drug and the lipid bilayer (Wong et al., 2013).

We hence assume that small molecular alterations in the lipid composition as well as the inclusion of chemical stabilizers (Chol, PEG) can critically influence the fluidity of the lipid bilayer and consequently the drug release of the encapsulated therapeutics.

3.3. *Effect of lipid composition on doxorubicin release: Cytotoxicity in human breast cancer cells*

To assess the release of doxorubicin and evaluate their potential as drug delivery systems in a physiological system, drug-free $DMPC_{100}$ and $DSPC_{100}$ liposomes, as well as their thermodynamically stable binary mixtures i.e., $DMPC_5$ and $DMPC_3$ liposomes, were selected for further studies. The selection was based on the doxorubicin release profiles (Fig. 6), to excluded the liposomes formulations with premature drug release (i.e., $DMPC_{0.2}$, $DMPC_{10}$) from further investigation.

Selected doxorubicin-loaded liposomes were tested for their cytotoxicity against a panel of breast cancer cells: the ER+/PR + hormone dependent MCF-7, the triple- negative MDA-MB 231 and the HER2 overexpressing BT-474 cells. The concentrations of liposomes used in this study were selected not to exceed 0.5 mg/mL of phospholipids, and to have the same initial concentration of loaded doxorubicin (155 μM), concentration typically used for cell studies (Abumanhal-Masarweh, 2019). Drug-free DMPC liposomes have been found to disrupt cancer cell membranes at ≥ 0.5 mM lipid concentrations, leading to premature cell death (Nagami et al., 2006). In addition, Nagami et al. have reported that short in length phospholipids (e.g. DMPC vs DPPC) and hybrid mixtures can induce significant apoptotic and necrotic activity in human leukaemia cells at a lipid concentration 0.3 mM, without the presence of

any anticancer agent (Heney, 2010). However, our previous findings (Gkionis et al., 2020), and in accordance with other research (Øverbye, 2017; Nagami et al., 2006; Wen, 2018), have shown that drug-free phosphatidylcholine liposomes did not alter significantly the cell viability at any concentration tested. This may be attributed to the fact that the liposomal formulations administered in our study did not exceed 0.5 mM of final lipid concentration. Based on these reports, and on the kinetics of liposomes internalisation in MCF-7 cells (***Supplementary Information*** **Fig SI.3**), we assessed cytotoxicity in the three cancer cell lines after 48 h of treatment exposure.

As expected, and similar to what is reported in the literature (Arif et al., 2013; Fang, 2014; You et al., 2018; Baciu et al., 2006); the cytotoxic profile of free doxorubicin over 48 h treatment was found to be highly potent (Fig. 7**A**), with IC50 values in the range of few hundred nM for both MCF-7 and MDA-231, and slightly higher for the more resistant BT474 cells (Table 7).

All the selected concentrations of doxorubicin-loaded liposomes had a similar toxicity across the breast cancer cell lines tested (Fig. 7**B-D**), with IC_{50} values higher than that of free doxorubicin and in the μM range (Table 7). $DMPC_{100}$ and $DSPC_{100}$ liposomes were both found to be less cytotoxic, with $DSPC_{100}$ liposomes slightly less potent than $DMPC_{100}$ liposomes. However, we might expect $DSPC_{100}$ liposomes to be more cytotoxic, based on their drug release rate (Fig. 6): $DSPC_{100}$ liposomes released almost all of the loaded doxorubicin after 48 h, whereas, $DMPC_{100}$ liposomes only released approximately 45% of the loaded drug at the same time point. DSPC/DMPC mixed liposomes exhibited rather comparable IC_{50} values, which were similar to those of free doxorubicin (Table 7), indicating a potent cytotoxic effect. During drug release studies, $DMPC_3$ liposomes released almost 60% of loaded doxorubicin at 48 h, whereas $DMPC_5$ liposomes released approximately 38% of doxorubicin (Fig. 6). However, these studies were not performed at the lower pH values typical of endosomes/lysosomes, which could explain a different release profile than the one observed at physiological pH of 7.4.

The internalisation rate of the different liposomal formulations could also explain the higher efficacy of doxorubicin-loaded DMPC-rich liposomes. In fact, PC(18:0) liposomes were reported to be endocytosed to a lesser extent by triple-negative breast cancer cells than their shorter in carbon-length PC(14:0) and PC(12:0) counterparts (Nagami et al., 2006). DMPC/Chol liposomes also reportedly exhibited significantly increased cellular uptake than HSPC/Chol liposomes in 4 T1 murine mammary gland tumour cells (Nagami et al., 2006). This would explain why $DSPC_{100}$ liposomes showed a lower cytotoxic effect when compared to $DMPC_{100}$, $DMPC_3$ and $DMPC_5$ liposomes (Table 7).

Another interesting finding, derived from Baciu's et al. research (Toroz and Gould, 2019), can further explain the potent cytotoxicity of the DMPC formulations. Cationic amphiphilic drugs, including doxorubicin, despite being actively transported or diffused through cell model membranes, can also cross cell membranes via phospholipidosis; an ester hydrolysis mechanism. Fragments of monochain-stranded phosphatidylcholines, produced following degradation by their cationic drug payload, form micellar structures that engulf and transport the drug molecules faster within the cytoplasmic compartment (Toroz and Gould, 2019). The relatively high partitioning of doxorubicin species to DMPC membranes[88], as well as the higher propensity of DMPC liposomes to fuse with biological membranes, could amplify this phenomenon by facilitating the transfer of higher doses of the drug intracellularly.

4. Conclusions

In the present study, we fabricated liposomes with different mixtures of phosphatidylcholines, encapsulating the anticancer agent doxorubicin using microfluidic technology. The use of microfluidics allowed the control of processing parameters for the fabrication of monodispersed PEGylated mixed DSPC/DMPC liposomes with size range < 200 nm. Liposomes were fabricated loading doxorubicin and characterized for drug delivery purposes, by varying the % mol DSPC content within the lipid composition. The microfluidic method was optimized to have a single-step production with not post-processing steps and ease of scale up, as compared to conventional batch methods.

Table 7
Cytotoxicity of doxorubicin loaded liposomal formulations in breast cancer cells: IC_{50} values of free doxorubicin drug and selected doxorubicin-loaded mixed phosphatidylcholine liposomes. Cell viability was determined by MTT assay after 48 h incubation with the treatment, and calculated as a percentage with respect to untreated controls. IC_{50} values were calculated using data from MTT assay; data are expressed as mean ± st.dev. (N = 2, biological replicates for all cell lines tested).

IC_{50} (μM) Treatment	MCF-7	MDA-MB-231	BT-474
Free Doxorubicin	0.97 ± 0.72	0.48 ± 0.14	1.86 ± 0.80
$DMPC_{100}$	3.10 ± 0.23	1.35 ± 0.11	4.20 ± 0.46
$DMPC_5$	1.04 ± 0.28	0.62 ± 0.18	1.40 ± 0.57
$DMPC_3$	0.93 ± 0.30	0.19 ± 0.01	1.42 ± 0.32
$DSPC_{100}$	4.75 ± 0.62	1.08 ± 0.08	7.72 ± 2.57

Among the formulations prepared, $DMPC_5$ and $DMPC_3$ liposomal formulations (containing up to 20% mol DSPC lipid) provided small, unilamellar vesicles that were characterized by high phase transition temperatures (T_g > 50℃), as well as prolonged *in vitro* drug release profiles (<40% overall release) over an incubation period of 48 h. These formulations, however, have shown a reduced encapsulation efficiency when compared to the other liposomal formulation. As multiple factors account for the differences in the fluidity of the lipid membranes (e.g. cholesterol content, final lipid concentration, PEGylation degree, drug partitioning) further drug release characterization may be required to better understand the dynamics of the system, such as release at different pH values and temperatures.

DMPC/DSPC mixed doxorubicin-loaded liposomes with distinctive drug release profiles were selected and tested *in vitro* against a panel of breast cancer cell lines. $DMPC_5$ and $DMPC_3$ liposomes were found to have cytotoxicity (i.e. IC_{50} values) similar to free doxorubicin, whereas the formulations composed of a single lipid species were less cytotoxic, and as expected. Further research using 3D tissue models would be useful to investigate the cellular internalization and anti-proliferative effects of the liposomes in a more relevant tumor associated microenvironment. This study reported on the use microfluidics for the single-step fabrication method for the fabrication of PCs mixed liposomes with controlled release profiles of chemotherapeutics, i.e. doxorubicin. Further optimisation on the formulation of drug-loaded liposomes using a single step automated system could not only provide a scalable manufacturing process, but also sustained system for the release of chemotherapeutics for cancer treatment.

CRediT authorship contribution statement

Leonidas Gkionis: Conceptualization, Methodology, Investigation, Validation, Formal analysis, Writing - original draft. **Harmesh Aojula:** Writing - review & editing. **Lynda K. Harris:** Writing - review & editing. **Annalisa Tirella:** Conceptualization, Formal analysis, Supervision, Writing - review & editing.

Declaration of Competing Interest

The authors declare that they have no known competing financial interests or personal relationships that could have appeared to influence the work reported in this paper.

Acknowledgments

Leonidas Gkionis is indebted to EPSRC for a PhD studentship as part of the GrapheneNOWNANO Doctoral Training Centre (EPSRC Grant No. EP/G03737X/1).

Appendix A. Supplementary data

Supplementary data to this article can be found online at https://doi.org/10.1016/j.ijpharm.2021.120711.

References

Kapitza, H. G., D. A. Ruppel, H. J. Galla, and E. S. Lateral diffusion of lipids and glycophorin in solid phosphatidylcholine bilayers. The role of structural defects. Biophys. J. 45, 577–587 (1984).

Peetla, C., Stine, A., Labhasetwar, V., 2009. Biophysical interactions with model lipid membranes: Applications in drug discovery and drug delivery. Mol. Pharm. 6, 1264–1276.

Akbarzadeh, A., et al., 2013. Liposome: classification, preparation, and applications. Nanoscale Res. Lett. 8, 1–9.

Juszkiewicz, K., Sikorski, A.F., Czogalla, A., 2020. Building blocks to design liposomal delivery systems. Int. J. Mol. Sci. 21, 1–22.

Chen, W., Duša, F., Witos, J., Ruokonen, S.K., Wiedmer, S.K., 2018. Determination of the Main Phase Transition Temperature of Phospholipids by Nanoplasmonic Sensing. Sci. Rep. 8, 1–11.

Chen, J., et al., 2013. Influence of lipid composition on the phase transition temperature of liposomes composed of both DPPC and HSPC. Drug Dev. Ind. Pharm. 39, 197–204.

Lokerse, W.J.M., et al., 2016. In depth study on thermosensitive liposomes: Optimizing formulations for tumor specific therapy and in vitro to in vivo relations. Biomaterials 82, 138–150.

Abri Aghdam, M., et al., 2019. Recent advances on thermosensitive and pH-sensitive liposomes employed in controlled release. J. Control. Release 315, 1–22.

Koynova, R., Caffrey, M., 1998. Phases and phase transitions of the phosphatidylcholines. BBA 1376, 91–145.

Michonova-Alexova, Ekaterina I, Istvan P., S. Component and State Separation in DMPC/DSPC Lipid Bilayers: A Monte Carlo Simulation Study. Biophys. J. 83, 1820–1833 (2002).

Briuglia, M.L., Rotella, C., McFarlane, A., Lamprou, D.A., 2015. Influence of cholesterol on liposome stability and on in vitro drug release. Drug Deliv. Transl. Res. 5, 231–242.

Kirby, C., Clarke, J., Gregoriadis, G., 1980. Effect of the cholesterol content of small unilamellar liposomes on their stability in vivo and in vitro. Biochem. J. 186, 591–598.

Bhattacharya, S., Saubhik, H., 2000. Interactions between cholesterol and lipids in bilayer membranes. Role of lipid headgroup and hydrocarbon chain-backbone linkage. BBA 1467, 39–53.

Soto-Arriaza, M.A., Olivares-Ortega, C., Quina, F.H., Aguilar, L.F., Sotomayor, C.P., 2013. Effect of cholesterol content on the structural and dynamic membrane properties of DMPC/DSPC large unilamellar bilayers. Biochim. Biophys. Acta - Biomembr. 1828, 2763–2769.

Raffy, S., Teissié, J., 1999. Control of lipid membrane stability by cholesterol content. Biophys. J . 76, 2072–2080.

Farzaneh, H., Ebrahimi, M., Mashreghi, M., Saberi, Z., 2018. A study on the role of cholesterol and phosphatidylcholine in various features of liposomal doxorubicin: From liposomal preparation to therapy. Int. J. Pharm. 551, 300–308.

Soto-Arriaza, M.A., Olivares-ortega, C., Quina, F.H., Aguilar, L.F., Sotomayor, C.P., 2013. Effect of cholesterol content on the structural and dynamic membrane properties of DMPC/ DSPC large unilamellar bilayers. Biochim. Biophys. Acta J. 1828, 2763–2769.

Shah, S., Dhawan, V., Holm, R., Nagarsenker, M.S., Perrie, Y., 2020. Liposomes: Advancements and innovation in the manufacturing process. Adv. Drug Deliv. Rev. 154, 101–122.

Carugo, D., Bottaro, E., Owen, J., Stride, E., Nastruzzi, C., 2016. Liposome production by microfluidics: potential and limiting factors. Sci. Rep. 6, 25876.

Feng, L., et al., 2018. Synthesis of Biomaterials Utilizing Microfluidic Technology. Genes (Basel) 9, 283.

Chiesa, E., et al., 2020. On-chip synthesis of hyaluronic acid-based nanoparticles for selective inhibition of CD44+ human mesenchymal stem cell proliferation. Pharmaceutics 12.

Cortés-Funes, H., Coronado, C., 2007. Role of anthracyclines in the era of targeted therapy. Cardiovasc. Toxicol. 7, 56–60.

Swain, S.M., et al., 2013. Definitive Results of a Phase III Adjuvant Trial Comparing Three Chemotherapy Regimens in Women With Operable, Node-Positive Breast Cancer: The NSABP B-38 Trial. J. Clin. Oncol. 31, 3197–3204.

Khan, D.R., Webb, M.N., Cadotte, T.H., Gavette, M.N., 2015. Use of Targeted Liposome-based Chemotherapeutics to Treat Breast Cancer. Breast cancer basic Clin. Res. 9, 1–5.

Belfiore, L., et al., 2018. Towards clinical translation of ligand-functionalized liposomes in targeted cancer therapy: Challenges and opportunities. J. Control. Release 277, 1–13.

Haran, G., Cohen, R., Bar, L.K., Barenholz, Y., 1993. Transmembrane ammonium sulfate gradients in liposomes produce efficient and stable entrapment of amphipathic weak bases. BBA 1151, 201–215.

Sur, S., Fries, A.C., Kinzler, K.W., Zhou, S., Vogelstein, B., 2014. Remote loading of preencapsulated drugs into stealth liposomes. PNAS 111, 1–6.

Barenholz, Y., 2012. Doxil® - The first FDA-approved nano-drug: Lessons learned. J. Control. Release 160, 117–134.

Russell, L.M., Hultz, M., Searson, P.C., 2018. Leakage kinetics of the liposomal chemotherapeutic agent Doxil: The role of dissolution, protonation, and passive transport, and implications for mechanism of action. J. Control. Release 269, 171–176.

Shibata, H., Izutsu, K.I., Yomota, C., Okuda, H., Goda, Y., 2015. Investigation of factors affecting in vitro doxorubicin release from PEGylated liposomal doxorubicin for the development of in vitro release testing conditions. Drug Dev. Ind. Pharm. 41, 1376–1386.

Gkionis, L., Campbell, R.A., Aojula, H., Harris, L.K., Tirella, A., 2020. Manufacturing drug co-loaded liposomal formulations targeting breast cancer: Influence of preparative method on liposomes characteristics and in vitro toxicity. Int. J. Pharm. 590, 119926.

Charles, J., Stewart, M., 1980. Colorirnetric Determination of Phospholipids Ferrothiocyanate. Anal. Biochem. 104, 10–14.

Schneider, C.A., Rasband, W.S., Eliceiri, K.W., Instrumentation, C., 2012. NIH Image to ImageJ: 25 years of Image Analysis. Nat. Methods 9, 671–675.

Chairatana, P., Chu, H., Castillo, P.A., Shen, B., 2016. Proteolysis triggers self-assembly and unmasks innate immune function of a human a-defensin peptide. Chem. Sci. 7, 1738–1752.

Kastner, E., Verma, V., Lowry, D., Perrie, Y., 2015. Microfluidic-controlled manufacture of liposomes for the solubilisation of a poorly water soluble drug. Int. J. Pharm. 485, 122–130.

Capretto, L., Carugo, D., Mazzitelli, S., Nastruzzi, C., Zhang, X., 2013. Microfluidic and lab-on-a-chip preparation routes for organic nanoparticles and vesicular systems for nanomedicine applications. Adv. Drug Deliv. Rev. 65, 1496–1532.

Pecora, R., 2000. Dynamic light scattering measurement of nanometer particles in liquids. J. Nanoparticle Res. 2, 123–131.

Carvalho, P.M., Felício, M.R., Santos, N.C., Gonçalves, S., Domingues, M.M., 2018. Application of light scattering techniques to nanoparticle characterization and development. Front. Chem. 6, 1–17.

Stetefeld, J., McKenna, S.A., Patel, T.R., 2016. Dynamic light scattering: a practical guide and applications in biomedical sciences. Biophys. Rev. 8, 409–427.

Ali, S., Minchey, S., Janoff, A., Mayhew, E., 2000. A differential scanning calorimetry study of phosphocholines mixed with paclitaxel and its bromoacylated taxanes. Biophys. J . 78, 246–256.

Trandum, C., Westh, P., Jørgensen, K., Mouritsen, O.G., 2000. A thermodynamic study of the effects of cholesterol on the interaction between liposomes and ethanol. Biophys. J . 78, 2486–2492.

Needham, D., Mcintosh, T.J., Evans, E., 1988. Thermomechanical and Transition Properties of Dimyristoylphosphatidylcholine/Cholesterol Bilayers. Biochemistry 27, 4668–4673.

Mcmullen, T.P.W., Mcelhaney, R.N., 1995. New aspects of the interaction of cholesterol with dipalmitoylphosphatidylcholine bilayers as revealed by high-sensitivity differential scanning calorimetry. BBA 1234, 90–98.

Corvera, E., Mouritsen, O.G., Singer, M.A., Zuckermann, M.J., 1992. The permeability and the effect of acyl-chain length for phospholipid bilayers containing cholesterol: theory and experiment. BBA - Biomembr. 1107, 261–270.

Redondo-Morata, L., Giannotti, M.I., Sanz, F., 2012. Influence of cholesterol on the phase transition of lipid bilayers: A temperature-controlled force spectroscopy study. Langmuir 28, 12851–12860.

Turjeman, K., et al., 2015. Nano-drugs based on nano sterically stabilized liposomes for the treatment of inflammatory neurodegenerative diseases. PLoS ONE 10, 1–25.

Mady, M.M., Shafaa, M.W., Abbase, E.R., Fahium, A.H., 2012. Interaction of Doxorubicin and Dipalmitoylphosphatidylcholine Liposomes. Cell Biochem. Biophys. 62, 481–486.

Alves, A.C., et al., 2017. Influence of doxorubicin on model cell membrane properties: Insights from in vitro and in silico studies. Sci. Rep. 7, 1–11.

Montenegro, L., Castelli, F., Sarpietro, M., 2018. Differential Scanning Calorimetry Analyses of Idebenone-Loaded Solid Lipid Nanoparticles Interactions with a Model of Bio-Membrane: A Comparison with In Vitro Skin Permeation Data. Pharmaceuticals 11, 138.

Fonseca, M.J., Van Winden, E.C.A., Crommelin, D.J.A., 1997. Doxorubicin induces aggregation of small negatively charged liposomes. Eur. J. Pharm. Biopharm. 43, 9–17.

Losada-Pérez, P., et al., 2015. Phase transitions of binary lipid mixtures: A combined study by adiabatic scanning calorimetry and quartz crystal microbalance with dissipation monitoring. Adv. Condens. Matter Phys. 2015.

Pokorny, A., Almeida, P.F.F., Vaz, W.L.C., 2001. Association of a Fluorescent Amphiphile with Lipid Bilayer Vesicles in Regions of Solid – Liquid-Disordered Phase Coexistence. Biophys. J . 80, 1384–1394.

Knoll, W., Ibel, K., Sackmannl, E., 1981. Small-Angle Neutron Scattering Study of Lipid Phase Diagrams by the Contrast Variation Methodt. Biochemistry 20, 6379–6383.

Nicolussi, A., Colonna, R., Massari, S., 1982. Effect of Lipid Mixing on the Permeability and Fusion of Saturated Lecithin Membraned. Biochemistry 21, 2134–2140.

Matubayasit, N., Shigematsu, T., Kamaya, H., Ueda, I., 1986. Miscibility of Phosphatidylcholine Binary Mixtures in UnUamellar Vesicles: Phase Equilibria. J. Membr. Biol. 90, 37–42.

Kraft, J.C., Freeling, J.P., Wang, Z., Ho, R.J.Y., 2014. Emerging research and clinical development trends of liposome and lipid nanoparticle drug delivery systems. J. Pharm. Sci. 103, 29–52.

Rocca, J., Liu, D., Lin, W., 2012. Are high drug loading nanoparticles the next step forward for chemotherapy? Nanomedicine (Lond) 7, 303–305.

Anderson, M. & Omri, A. The Effect of Different Lipid Components on the in Vitro Stability and Release Kinetics of Liposome Formulations. Drug Deliv. J. Deliv. Target. Ther. Agents 11, 33–39 (2004).

Ali, M.H., Moghaddam, B., Kirby, D.J., Mohammed, A.R., Perrie, Y., 2013. The role of lipid geometry in designing liposomes for the solubilisation of poorly water soluble drugs. Int. J. Pharm. 453, 225–232.

Dan, N., 2007. Lipid tail chain asymmetry and the strength of membrane-induced interactions between membrane proteins. BBA 1768, 2393–2399.
Ann, S., Edwards, K., Karlsson, G. & et al. Formation of transition metal – doxorubicin complexes inside liposomes. Biochim. Biophys. Acta 1565, 41–54 (2002).
Farzaneh, H., et al., 2018. A study on the role of cholesterol and phosphatidylcholine in various features of liposomal doxorubicin: From liposomal preparation to therapy. Int. J. Pharm. 551, 300–308.
Subczynski, W., Pasenkiewicz-Gierula, M., Widomska, J., Mainali, L., Raguz, M., 2017. High cholesterol/low cholesterol: Effects in biological membranes Review. Cell Biochem. Biophys. 75, 369–385.
Wallace, S.J., Li, J., Nation, R.L., Boyd, B.J., 2012. Drug release from nanomedicines: Selection of appropriate encapsulation and release methodology. Dug Deliv Transl Res 2, 284–292.
Mohammed, A.R., Weston, N., Coombes, A.G.A., Fitzgerald, M., Perrie, Y., 2004. Liposome formulation of poorly water soluble drugs: optimisation of drug loading and ESEM analysis of stability. Int. J. Pharm. 285, 23–34.
Swenson, C.E., Perkins, W.R., Roberts, P., Janoff, A.S., 2001. Liposome technology and the development of Myocet^{TM} (liposomal doxorubicin citrate). The Breast 10, 1–7.
Cohen, A.A., 2014. Mathematical Models of Drug Dissolution: A Review. Sch. Acad. J. Pharm. 3, 388–396.
Muderhwa, J.M., Matyas, G.R., Spitler, L.E., Alving, C.R., 1999. Oil-in-water liposomal emulsions: Characterization and potential use in vaccine delivery. J. Pharm. Sci. 88, 1332–1339.
P.L. Chong, M. O. Fluorescence studies of the existence and functional importance of regular distributions in liposomal membranes. Soft Matter 2, 85–108 (2004).
Lasic, D.D., et al., 1995. Transmembrane gradient driven phase transitions within vesicles: lessons for drug delivery. BBA 1239, 145–156.
Santos, N. Dos, et al., 2004. pH gradient loading of anthracyclines into cholesterol-free liposomes: enhancing drug loading rates through use of ethanol. BBA 1661, 47–60.
Gallois, L., Fiallo, M., Laigle, A., Priebe, W., Garnier-Suillerot, A., 1996. The overall partitioning of anthracyclines into phosphatidyl-containing model membranes depends neither on the drug charge nor the presence of anionic phospholipids. Eur. J. Biochem. 241, 879–887.
Modi, S., Anderson, B.D., 2013. Determination of drug release kinetics from nanoparticles: Overcoming pitfalls of the dynamic dialysis method. Mol. Pharm. 10, 3076–3089.
C. Allen, N. Dos Santos, R. Gallagher, G. N. C. Chiu, Y. S. Controlling the physical behavior and biological performance of liposome formulations through use of surface grafted poly (ethylene glycol). Biosci. Rep. 22, 225–250 (2002).
Viitala, Lauri, Saija Pajari, L.G., et al., 2019. Shape and Phase Transitions in a PEGylated Phospholipid System. Langmuir 35, 3999–4010.
Rissanen, S., et al., 2014. Effect of PEGylation on Drug Entry into Lipid Bilayer. J. Phys. Chem. 118, 144–151.
Wong, F.C., Woo, C.C., Hsu, A., Tan, B.K.H., 2013. The Anti-Cancer Activities of Vernonia amygdalina Extract in Human Breast Cancer Cell Lines Are Mediated through Caspase-Dependent and p53-Independent Pathways. PLoS ONE 8, 78021.
Abumanhal-Masarweh, H., et al., 2019. Tailoring the lipid composition of nanoparticles modulates their cellular uptake and affects the viability of triple negative breast cancer cells. J. Control. Release 307, 331–341.
Nagami, H., Nakano, K., Ichihara, H. & et al. Two methylene groups in phospholipids distinguish between apoptosis and necrosis for tumor cells. Bioorg. Med. Chem. Lett. 16, 782–785 (2006).
Heney, M., et al., 2010. Effectiveness of liposomal paclitaxel against MCF-7 breast cancer cells. Can. J. Physiol. Pharmacol. 88, 1172–1180.
Øverbye, A., et al., 2017. Ceramide-containing liposomes with doxorubicin: Time and cell-dependent effect of C6 and C12 ceramide. Oncotarget 8, 76921–76934.
Wen, S. hsuan, Su, S. chiang, Liou, B. huang, Lin, C. hao & Lee, K. rong. Sulbactam-enhanced cytotoxicity of doxorubicin in breast cancer cells. Cancer Cell Int. 18, 1–18 (2018).
Arif, I.S., Hooper, C.L., Greco, F., Williams, A.C., Boateng, S.Y., 2013. Increasing doxorubicin activity against breast cancer cells using PPARγ-ligands and by exploiting circadian rhythms. Br. J. Pharmacol. 169, 1178–1188.
Fang, X.J., et al., 2014. Doxorubicin induces drug resistance and expression of the novel CD44st via NF-κB in human breast cancer MCF-7 cells. Oncol. Rep. 31, 2735–2742.
You, Y., Xu, Z., Chen, Y., 2018. Doxorubicin conjugated with a trastuzumab epitope and an MMP-2 sensitive peptide linker for the treatment of HER2-positive breast cancer. Drug Deliv. 25, 448–460.
Baciu, M., Sebai, S.C., Ces, O., Mulet, X., Clarke, J.A., Shearman, G.C., Law, R.V., Templer, R.H., Plisson, C., Gee, A., 2006. Degradative transport of cationic amphiphilic drugs across phospholipid bilayers. Philos. Trans. R. Soc. 364, 2597–2614.
Toroz, D., Gould, I.R., 2019. A computational study of Anthracyclines interacting with lipid bilayers: Correlation of membrane insertion rates, orientation effects and localisation with cytotoxicity. Sci. Rep. 9, 1–12.